Since January 2020 Elsevier has created a COVID-19 resource centre with free information in English and Mandarin on the novel coronavirus COVID-19. The COVID-19 resource centre is hosted on Elsevier Connect, the company's public news and information website.

Chaos, Solitons and Fractals 157 (2022) 111954

Contents lists available at ScienceDirect

Chaos, Solitons and Fractals

Nonlinear Science, and Nonequilibrium and Complex Phenomena

journal homepage: www.elsevier.com/locate/chaos

Fractional order modelling of omicron SARS-CoV-2 variant containing heart attack effect using real data from the United Kingdom

Fatma Özköse[a], Mehmet Yavuz[b,c,*], M. Tamer Şenel[a], Rafla Habbireeh[d,e]

[a] Erciyes University, Department of Mathematics, Faculty of Science, Kayseri, Turkey
[b] Department of Mathematics and Computer Sciences, Faculty of Science, Necmettin Erbakan University, Konya, 42090, Turkey
[c] Department of Mathematics, College of Engineering, Mathematics and Physical Sciences, University of Exeter, TR10, Cornwall, United Kingdom
[d] Institute of Science, Erciyes University, Kayseri 38039, Turkey
[e] Department of Mathematics, Faculty of Science, Misurata University, Misurata, Libya

ARTICLE INFO

Article history:
Received 23 January 2022
Revised 24 February 2022
Accepted 24 February 2022
Available online 28 February 2022

Keywords:
Fractional order derivative
Omicron SARS-CoV-2 variant
Heart attack
Parameter estimation with real data
Sensitivity analysis
Memory trace and hereditary traits

ABSTRACT

In this study, a new approach to COVID-19 pandemic is presented. In this context, a fractional order pandemic model is developed to examine the spread of COVID-19 with and without Omicron variant and its relationship with heart attack using real data from the United Kingdom. In the model, heart attack is adopted by considering its relationship with the quarantine strategy. Then, the existence, uniqueness, positivity and boundedness of the solution are studied. The equilibrium points and their stability conditions are achieved. Subsequently, we calculate the basic reproduction number (the virus transmission coefficient) that simply refers to the number of people, to whom an infected person can make infected, as $R_0 = 3.6456$ by using the next generation matrix method. Next, we consider the sensitivity analysis of the parameters according to R_0. In order to determine the values of the parameters in the model, the least squares curve fitting method, which is one of the leading methods in parameter estimation, is benefited. A total of 21 parameter values in the model are estimated by using real Omicron data from the United Kingdom. Moreover, in order to highlight the advantages of using fractional differential equations, applications related to memory trace and hereditary properties are given. Finally, the numerical simulations are presented to examine the dynamic behavior of the system. As a result of numerical simulations, an increase in the number of people who have heart attacks is observed when Omicron cases were first seen. In the future, it is estimated that the risk of heart attack will decrease as the cases of Omicron decrease.

1. Introduction

Coronavirus disease (COVID-19) is a recent contagious disease caused by the SARS-COV-2 virus and one of the most famous symptoms of this disease is the emergence of breathing problems from mild to moderate where sometimes the person with this disease may recover without the need for treatment. There are symptoms of infection with this virus, including what is common, such as fever, cough, loss of sense of taste and smell, and what is less common, such as sore throat, headache, diarrhea, the appearance of a rash, redness in the eyes, and some may develop serious symptoms of this disease such as difficulty or shortness of breath, loss of ability to speak or move and pain in the chest, so the patient at this case, they need medical care. Older adults and those who suffer from chronic diseases such as cardiovascular disease, diabetes, chronic respiratory disease, cancer are more likely to develop serious illnesses. Anyone can contract COVID-19 disease and become seriously ill or die at any age. In 2020, WHO announced that the Coronavirus that has been caused the COVID-19 disease, and infected more than 110,000 people around the world since December 2019, it is a “pandemic” spreading around the world. The total diagnoses worldwide are 404910528, of which 52,616,197 have been vaccinated and 5,783,776 have died (https://covid19.who.int/).

All viruses, including coronavirus, change over time. Most changes have little or no effect on the characteristics of the virus. However, some of these changes may affect the characteristics of the virus, such as how easily it spreads, the degree and severity of

* Corresponding author at: Department of Mathematics and Computer Sciences, Faculty of Science, Necmettin Erbakan University, Konya, 42090, Turkey.
E-mail addresses: fpeker@erciyes.edu.tr (F. Özköse), M.Yavuz@exeter.ac.uk (M. Yavuz), senel@erciyes.edu.tr (M.T. Şenel), r.habbireeh@sci.misuratau.edu.ly (R. Habbireeh).

https://doi.org/10.1016/j.chaos.2022.111954

the disease associated with it, or the performance of vaccines, therapeutic drugs, diagnostic tools, or other public health and social measures. Recently, scientists discovered the new variant "Omicron" in South Africa, where data emerged showing the presence of samples of a new variant with similar and different characteristics from "Omicron". Scientists found the new form of the "Omicron Plus" variant in 3 countries: South Africa, Australia, and the United States, according to data published on the "GitHub" website, which researchers use to share information about the Coronavirus. Many of the mutations that were discovered in "Omicron" appear in the new variant, but not all of them, and according to scientists, the new variant has many unique mutations. As a result of great similarity with the variant "Omicron", scientists called the new version "BA.2", and the first is called "BA.1". Some scientists and the media have dubbed the new variant the "ghost omicron" for its ability to mislead (PCR) tests about the truth of which variant it belongs to. The danger of the matter is that tracking the spread of "Omicron" will become more difficult, at a time when the process of monitoring the mutation is critical to understanding its nature.

One of the best ways to prevent the spread of this disease is isolation, because sometimes the symptoms of the disease may not appear on the patient, which causes the virus to transmit more quickly. Mental health specialists agree that the quarantine (isolation) imposed on more than a billion people around the world due to the Coronavirus pandemic, is neither an easy matter nor a matter to be underestimated, as it is an exceptional and unprecedented measure that restricts individual freedoms even in democratic countries. This situation causes psychological problems for many people, especially for those who fail to deal positively with this circumstance. In addition, the elderly with chronic heart disease are the most affected by the Coronavirus, due to low immunity, and having to sit at home for a long time. According to doctors, these patients should protect themselves more carefully during the phase of combating the Corona epidemic, and that neglecting to take medicines regularly causes various complaints. Headache and fatigue due to increased blood pressure are some of the main symptoms experienced by these patients. Coronary artery patients may also suffer from chest pain during the home quarantine period as a result of not exercising regularly during that period, as shortness of breath is one of the most prominent symptoms faced by coronary artery patients and heart failure patients. Doctors stressed that cardiovascular patients should strive to live in healthy ways, especially during the phase of fighting the epidemic and quarantine, because neglecting to take medications for chronic heart disease patients for a day may cause conditions such as heart attack, stroke, even death. Conditions must be created to end this pandemic before it is too late, and more people die. Although there are many medical treatments that are currently being applied, the most important of which is taking the vaccine to prevent the disease or greatly reduce the symptoms and negative effects that it causes to the patient, any treatment method has not yet been found that can eliminate the disease.

It is very important when facing any epidemic to predict what will happen in the future, know how to limit the spread of this epidemic, and give the necessary instructions to deal with it before it is too late. Many researchers from different disciplines have contributed to the prediction, study, and development of important ways to combat COVID-19. Previously, many mathematical models were used to model many epidemics. Indeed, it has been noted that these models are effective tools for treating and eliminating diseases, so it is still to this day that diseases are modeled mathematically to know how to deal with them [1,2]. Despite the success of the results resulting from the use of equations of the integer-order, to some extent, the results resulting from the use of equations of the fractional-order are still better in terms of their relationship to reality more when it represents real phenomena. What distinguishes modeling using FDEs are some of the properties that exist in these types of equations without others, such as the property of repeating operations and the fact that it contains non-local properties, these properties make the current state of the model that was made by this type of equations commensurate with the previous states and the following states as well. Many phenomena that occur in our real world are described better by FDEs, e.g. the heat equation, telegraph equation, social systems, medical imaging, pollution control, cancer dynamics, infectious diseases, and a lossy electric transmission line. FDEs are often associated with systems that have hereditary properties.

Additionally, FDE contributes significantly to reducing the possible errors that may arise from some parameters that should be neglected in mathematical modeling. The uniqueness of FDEs makes them well suited to studying many diseases by modeling them using FDEs. For example, Baleanu [3] et al. introduced a new comparative study on the general fractional model of COVID-19 with isolation and quarantine effects. Their comparative study indicates that a particular case of general fractional formula provides a better fit to the real data compared to the other classical and fractional models. Jajarmi et al. [4] presented a new and general fractional formulation to investigate the complex behaviors of a capacitor microphone dynamical system. According to their results, various features of the capacitor microphone under study are discovered due to the flexibility in choosing the kernel, unlike the previous mathematical formalism. In study [5], Baleanu et al. analyzed a novel fractional chaotic system including quadratic and cubic nonlinearities. They found that the new model portrays both chaotic and nonchaotic behaviors for different values of the fractional order, so that the lowest order in which the system remains chaotic is found via the numerical simulations. Sene [6] investigated the second-grade fluid with Newtonian heating under Caputo fractional derivative. Erturk et al. [7] studied a novel fractional-order Lagrangian to describe motion of beam on nanowire. Amar Nath Chatterjee et al. [8] proposed a model of COVID-19 infection of epithelial cells using the Caputo–Fabrizio derivative. Özköse et al. [9] studied the interactions between COVID-19 and diabetes using real data from Turkey. Allegretti et al. [10] investigated how the vaccination rate and the fraction of avoided contacts affect the population dynamics on a COVID-19 model. Musa et al., [11] proposed a mathematical model to study the transmission dynamics of COVID-19 in Nigeria. Memon et al., [12] proposed a new model related with outbreak of coronavirus with major focus given on the dynamics of quarantined, infected and isolated classes. Peter et al., [13] constructed a new mathematical model to investigate the recent outbreak of the coronavirus disease (COVID-19) in Pakistan. Naik et al. [14] described a mathematical model of the COVID-19 pandemic using Caputo, Caputo–Fabrizio and Atangana–Baleanu operators and studied the possible direction of the pandemic in Pakistan with real data. Jajarmi et al. [15], investigated the asymptotic behavior of immunogenic tumor dynamics based on a new fractional model constructed by the concept of general fractional operators. The work carried out in this study makes the research rich in the new direction of Fractional Calculus as well as its applications. Öztürk et al. [16] studied the stability of fractional-order model of tumor-immune system interaction, Hammouch et al. [17] studied numerical solutions and synchronization of a variable-order fractional chaotic system, Naik et al. [18] proposed a dynamic fractional-order HIV-1 model which includes interactions between tumor cells, healthy lymphocytes, and virus-infected lymphocytes resulting in chaotic behavior, Özköse et al. [19] examined the effect of chemotherapy on tumor cells and stem cells over time by using Caputo fractional derivative. In the following references, there are various studies using fractional-order models in different fields of science. Among

them, in Akgül et al. [20], the authors pointed out some interesting applications related to COVID-19. In [21], the authors constructed a new fractional-order mathematical model which considers population dynamics among tumor cells-macrophage cells-active macrophage cells, and host cells involving the Caputo fractional derivative. In [22], Akgul et al. investigated the epidemiological analysis of a fractional order COVID-19 model with Mittag–Leffler kernel. In [23], Joshi and Jha developed a mathematical calcium model in the form of the Hilfer fractional reaction-diffusion equation for Parkinson's disease to examine the calcium diffusion in the cells. In [24], the authors developed a new fractional order derivative with a non-singular kernel and they applied it to the heat transfer model. In another paper [25], Bonyah et al. took into account the listeriosis disease by adopting fractal-fractional operators. Kumar and Erturk [26] used two different fractional order numerical methods to examine the dynamics of the cholera disease. Uçar et al. considered a fractional order SAIDR model by using the Atangana–Baleanu derivative in Uçar et al. [27].

Impact of COVID-19 on cardiovascular complications and increased mortality in patients with recent cardiovascular disease (CVD) mentioned in many medical studies [28–30]. The virus invades heart muscle cells by binding to angiotensin-converting enzyme 2 cell surface, resulting in myocardial injury and elevation of troponin I levels. In particular, COVID-19 Infection can lead to myocarditis, vasculitis, and arrhythmias. It has been observed that more cardiovascular patients with COVID-19 died than those who survived. Moreover, some studies have highlighted that for patients with COVID-19, the higher mortality rate is for those people with chronic diseases.

The main objective of this work is to know the extent of the spread of the COVID-19 epidemic and the Omicron variant, to predict in the future what could happen and how to reduce the spread of this disease, and to know the impact of COVID-19 quarantine on heart patients. We present a new model showing how COVID-19 spreads, mathematical modeling of the dynamics of heart disease, and then the possible effects of quarantined patients with heart disease. We used fractional derivatives under the Caputo derivative.

At first, we discuss the formulation of the model and then show the existence and uniqueness of the solution to this model. Then, we have found the basic reproduction number and equilibria to determine the parameters that will limit the spread of the pandemic. In addition, by using real Omicron data taken from the U.K., we have fitted the parameters we use in the numerical simulation to be as close to reality as possible using the prediction method for these parameters. We have also performed a sensitivity analysis to analyze those factors that led to the increased prevalence of this disease. Finally, the COVID-19 and heart attack model have been solved using the Caputo operator numerically, and the graphical effect of different values of fractional order and different parameters has been shown.

The sections in the paper are arranged as follows: In Section 2, we have presented the most important definitions of fractional calculus. The fractional-order model has been given in Section 3. Existence and uniqueness of the model solution are presented in Section 4. In Section 5, positivity and boundedness of the solution and the stability of the equilibrium points model are given. Also, the basic reproduction number has been calculated. The sensitivity analysis has been investigated according to the parameters to study the extent of its effect on the reproduction number in the Section 6. The parameter estimation method is studied in Section 7. The numerical method of the proposed model is given in Section 8. In Section 9, the memory effects and hereditary traits are discussed. In Section 10, the numerical solutions for our model are presented by using the Adams–Bashforth Moulton method for the fitted parameter values in Table 1. In Section 11, the effect of memory tracking on populations of the model has been shown. Finally, a summary of the present work is presented in Section 12.

2. Preliminaries

In this section we have mentioned the definitions of fractional calculus used in this paper.

Definition 1 [31]. The fractional integral of order $\vartheta > 0$, of the function $f(t)$, $t > 0$ is given by

$$I^{\vartheta} f(t) = \int_0^t \frac{(t-s)^{\vartheta-1}}{\Gamma(\vartheta)} f(s)ds,$$

and the fractional derivative of order $\vartheta \in (n-1, n)$ of $f(t)$, $t > 0$ is given by

$$D^{\vartheta} f(t) = I^{n-\vartheta} D^n f(t) \left(D = \frac{d}{dt} \right),$$

where $\vartheta > 0$ and $\Gamma(.)$ is the Gamma function.

Table 1
Parameter values used for numerical analysis.

Par.	Meaning	Value	Source
Λ^{ϑ}	Recruitment rate	$2.2996e+03$	Estimated
μ^{ϑ}	The natural death rate	$3.3608e-05$	Estimated
μ_2^{ϑ}	The death rate from heart attack	0.4105	Fitted
γ_1^{ϑ}	The rate of susceptible individuals who have been in quarantine	$1.0063e-04$	Fitted
γ_2^{ϑ}	The probability of developing heart attack of susceptible individuals	$1.0003e-04$	Fitted
γ_3^{ϑ}	The probability of developing heart attack of recovered individuals	0.3535	Fitted
δ_1^{ϑ}	The mortality rate due to complications	0.9	Fitted
δ_2^{ϑ}	The probability of developing heart attack of infected individuals in I class	0.8847	Fitted
δ_3^{ϑ}	The mortality rate due to complications	0.0322	Fitted
δ_4^{ϑ}	The probability of developing heart attack of infected individuals in O class	0.0322	Fitted
β_1^{ϑ}	Rate of disease transmission through contact with E class	0.4553	Fitted
β_2^{ϑ}	Rate of disease transmission through contact with I class	0.0129	Fitted
β_3^{ϑ}	Rate of disease transmission through contact with O class	$1.0147e-04$	Fitted
α_1^{ϑ}	Screening rate of individuals infected with COVID-19	0.0093	Fitted
α_2^{ϑ}	The rate of people recovered from the I class	0.8841	Fitted
α_3^{ϑ}	The rate of people recovered from the O class	0.0322	Fitted
σ^{ϑ}	Screening rate of individuals infected with Omicron variant	$1.0002e-04$	Fitted
τ^{ϑ}	The probability of developing heart attack of S class due to quarantine	0.2747	Fitted
θ_1^{ϑ}	The rate of quarantine of people infected without symptoms	0.0103	Fitted
θ_2^{ϑ}	The rate of quarantine of people infected with COVID-19	0.9	Fitted
θ_3^{ϑ}	The rate of quarantine of people infected with Omicron variant	0.0322	Fitted
$\varepsilon_1^{\vartheta}$	Recognition of non-Omicron variant infection	0.1012	Fitted
$\varepsilon_2^{\vartheta}$	Recognition of Omicron variant infection	$1.0000e-04$	Fitted

Definition 2 ([31]). The Caputo fractional derivative of order $\vartheta > 0$ of a function $f : (0, \infty) \to \mathcal{R}$ is given by

$$ {}_0^C D_t^{\vartheta} f(t) = \begin{cases} \frac{1}{\Gamma(n-\vartheta)} \int_0^t \frac{(d/d\tau)^n f(\tau)}{(t-\tau)^{\vartheta-n+1}} d\tau, & 0 \le n-1 < \vartheta < n, \quad n = [\vartheta], \ n \in N, \\ \left(\frac{d}{dt}\right)^n f(t), & \vartheta = n, \ n \in N. \end{cases} \tag{1} $$

Definition 3 ([31]). The Laplace transform (LT) of the Caputo operator of the function f(t) of order $\vartheta > 0$ is defined by

$$ L[{}_0^C D_t^{\vartheta} f(t)] = s^{\vartheta} f(s) - \sum_{v=0}^{n-1} f^v(0) s^{\vartheta-v-1}. \tag{2} $$

Definition 4 ([31]). The Laplace transform (LT) of the function $f(t) = t^{\vartheta_1-1} E_{\vartheta,\vartheta_1}(\pm\omega t^{\vartheta})$ is defined as

$$ L[t^{\vartheta_1-1} E_{\vartheta,\vartheta_1}(\pm\omega t^{\vartheta})] = \frac{s^{\vartheta-\vartheta_1}}{s^{\vartheta} \pm \omega}, \tag{3} $$

where $E_{\vartheta,\vartheta_1}$ is Mittag–Leffler function.

Theorem 1 ([32,33]). *Consider the following fractional-order system:*

$$ \frac{d^{\vartheta} x}{dt^{\vartheta}} = f(x), \quad x(0) = x_0, \tag{4} $$

with $x \in R^n$ and $\vartheta \in (0,1]$. The equilibrium points of the system (4) are solutions to the equation $f(X^*) = 0$, and these equilibrium points:

(1) *Asymptotically stable $\iff$ all the eigenvalues λ_i, $i = 1, 2, \ldots, n$ of the Jacobian matrix $J(X^*)$ satisfy that $|arg(\lambda_i)| > \frac{\vartheta\pi}{2}$.*
(2) *Stable $\iff$ it is asymptotically stable or the eigenvalues λ_i, $i = 1, 2, \ldots, n$ of $J(X^*)$ that satisfy $|arg(\lambda_i)| = \frac{\vartheta\pi}{2}$ if have the same geometric multiplicity and algebraic multiplicity.*
(3) *Unstable $\iff$ eigenvalues λ_i for some $i = 1, 2, \ldots, n$ of $J(X^*)$ satisfy $|arg(\lambda_i)| < \frac{\vartheta\pi}{2}$.*

3. Mathematical modelling

The representation of infectious diseases using mathematical models helps us predict the extent and severity of these diseases. Strategies to treat many diseases and limit their spread can be developed using mathematical models. The disease COVID-19, which has been spreading for more than two years to our time now, has been represented by different mathematical models, including what shows the extent of its negative impact on several other diseases. Where some of these models took into account the vaccine and some of the models took into account the quarantine that was applied to prevent the spread of the disease. Some models also show the effect of COVID-19 on different types of diseases, the most important of which are chronic diseases such as diabetes [9]. In this work, a model has been created to study the side effects of COVID-19 on patients with heart attack disease. To examine the spread of COVID-19 with and without Omicron variant, we consider seven sub-populations as susceptible, exposed, COVID-infected without Omicron, omicron-infected, recovered, quarantined, having a heart attack. A person who is healthy and vulnerable is denoted by S, a person who has not yet been infected and who is still in the latent period denoted by E, a person infected with COVID-19 is denoted by I, a person infected with omicron variant that is more transmissible variant of the COVID virus denoted by O, recovered population R, isolated K, and those who have had a heart attack H. The proposed fractional-order model as follows:

$$ \begin{aligned} {}_0^C D_t^{\vartheta} S &= \Lambda^{\vartheta} - \left(\mu^{\vartheta} + \gamma_1^{\vartheta} + \gamma_2^{\vartheta}\right) S - \beta_1^{\vartheta} \frac{SE}{N} - \beta_2^{\vartheta} \frac{SI}{N} - \beta_3^{\vartheta} \frac{SO}{N}, \\ {}_0^C D_t^{\vartheta} E &= \beta_1^{\vartheta} \left(1 - \varepsilon_1^{\vartheta} - \varepsilon_2^{\vartheta}\right) \frac{SE}{N} - \left(\mu^{\vartheta} + \alpha_1^{\vartheta} + \theta_1^{\vartheta} + \sigma^{\vartheta}\right) E, \\ {}_0^C D_t^{\vartheta} I &= \beta_1^{\vartheta} \varepsilon_1^{\vartheta} \frac{SE}{N} + \beta_2^{\vartheta} \frac{SI}{N} + \alpha_1^{\vartheta} E - \left(\mu^{\vartheta} + \alpha_2^{\vartheta} + \theta_2{}^{\vartheta} + \delta_1^{\vartheta} + \delta_2^{\vartheta}\right) I, \\ {}_0^C D_t^{\vartheta} O &= \beta_1^{\vartheta} \varepsilon_2^{\vartheta} \frac{SE}{N} + \beta_3^{\vartheta} \frac{SO}{N} + \sigma^{\vartheta} E - \left(\mu^{\vartheta} + \alpha_3^{\vartheta} + \theta_3{}^{\vartheta} + \delta_3^{\vartheta} + \delta_4^{\vartheta}\right) O, \\ {}_0^C D_t^{\vartheta} R &= \alpha_2^{\vartheta} I + \alpha_3^{\vartheta} O - \gamma_3^{\vartheta} R - \mu^{\vartheta} R, \\ {}_0^C D_t^{\vartheta} K &= (1 - \tau^{\vartheta}) \gamma_1^{\vartheta} S + \theta_1^{\vartheta} E + \theta_2^{\vartheta} I + \theta_3^{\vartheta} O - \mu^{\vartheta} K, \\ {}_0^C D_t^{\vartheta} H &= (\gamma_2^{\vartheta} + \tau^{\vartheta} \gamma_1^{\vartheta}) S + \delta_2^{\vartheta} I + \delta_4^{\vartheta} O + \gamma_3^{\vartheta} R - (\mu_2^{\vartheta} + \mu^{\vartheta}) H, \end{aligned} \tag{5} $$

with initial condition

$$ S(0) = S_0 \ge 0, E(0) = E_0 \ge 0, I(0) = I_0 \ge 0, O(0) = O_0 \ge 0, R(0) = R_0 \ge 0, K(0) = K_0 \ge 0, H(0) = H_0 \ge 0. $$

The biological meanings of the parameters in model (5) is given by the next Table.

4. Existence and uniqueness

Consider the system (5) with the initial conditions $S(0) = S_0, E(0) = E_0, I(0) = I_0, O(0) = O_0, R(0) = R_0, K(0) = K_0, H(0) = H_0$. System (5) can be written in the following form:

$$ \begin{aligned} {}_0^C D_t^{\vartheta} X(t) &= B_1 X(t) + S(t) B_2 X(t) + E(t) B_3 X(t) + I(t) B_4 X(t) + O(t) B_5 X(t), \\ X(0) &= X_0, \end{aligned} \tag{6} $$

where

$$X(t)=\begin{pmatrix}S(t)\\E(t)\\I(t)\\O(t)\\R(t)\\K(t)\\H(t)\end{pmatrix},\quad X(0)=\begin{pmatrix}S(0)\\E(0)\\I(0)\\O(0)\\R(0)\\K(0)\\H(0)\end{pmatrix},$$

$$B_1=\begin{pmatrix}-A_1 & 0 & 0 & 0 & 0 & 0 & 0\\ 0 & -A_2 & 0 & 0 & 0 & 0 & 0\\ 0 & \alpha_1^{\vartheta} & -A_3 & 0 & 0 & 0 & 0\\ 0 & \sigma^{\vartheta} & 0 & A_4 & 0 & 0 & 0\\ 0 & 0 & \alpha_2^{\vartheta} & \alpha_3^{\vartheta} & -(\mu^{\vartheta}+\gamma_3^{\vartheta}) & 0 & 0\\ (1-\tau^{\vartheta})\gamma_1^{\vartheta} & \theta_1^{\vartheta} & \theta_2^{\vartheta} & \theta_3^{\vartheta} & 0 & -\mu^{\vartheta} & 0\\ (\gamma_2^{\vartheta}+\tau^{\vartheta}\gamma_1^{\vartheta}) & 0 & \delta_2^{\vartheta} & \delta_4^{\vartheta} & \gamma_3^{\vartheta} & 0 & -(\mu_2^{\vartheta}+\mu^{\vartheta})\end{pmatrix},$$

$$B_2=\begin{pmatrix}0 & \frac{-\beta_1^{\vartheta}}{N} & \frac{-\beta_2^{\vartheta}}{N} & \frac{-\beta_3^{\vartheta}}{N} & 0 & \dots & 0\\ 0 & 0 & 0 & 0 & 0 & \dots & 0\\ 0 & \frac{\beta_1^{\vartheta}\varepsilon_1^{\vartheta}}{N} & 0 & 0 & 0 & \dots & 0\\ 0 & 0 & 0 & 0 & 0 & \dots & 0\\ 0 & 0 & 0 & 0 & 0 & \dots & 0\\ 0 & 0 & 0 & 0 & 0 & \dots & 0\\ 0 & 0 & 0 & 0 & 0 & \dots & 0\end{pmatrix},\quad B_3=\begin{pmatrix}0 & 0 & \dots & 0\\ \frac{\beta_1^{\vartheta}(1-\varepsilon_1^{\vartheta}-\varepsilon_2^{\vartheta})}{N} & 0 & \dots & 0\\ 0 & 0 & \dots & 0\\ \frac{\beta_1^{\vartheta}\varepsilon_2^{\vartheta}}{N} & 0 & \dots & 0\\ 0 & 0 & \dots & 0\\ 0 & 0 & \dots & 0\\ 0 & 0 & \dots & 0\end{pmatrix},$$

$$B_4=\begin{pmatrix}0 & 0 & \dots & 0\\ 0 & 0 & \dots & 0\\ \frac{\beta_2^{\vartheta}}{N} & 0 & \dots & 0\\ 0 & 0 & \dots & 0\\ 0 & 0 & \dots & 0\\ 0 & 0 & \dots & 0\\ 0 & 0 & \dots & 0\end{pmatrix},\quad B_5=\begin{pmatrix}0 & 0 & \dots & 0\\ 0 & 0 & \dots & 0\\ 0 & 0 & \dots & 0\\ \frac{\beta_3^{\vartheta}}{N} & 0 & \dots & 0\\ 0 & 0 & \dots & 0\\ 0 & 0 & \dots & 0\\ 0 & 0 & \dots & 0\end{pmatrix},\quad \phi=\begin{pmatrix}\Lambda^{\vartheta}\\0\\0\\0\\0\\0\\0\end{pmatrix},$$

where $A_1=\mu^{\vartheta}+\gamma_1^{\vartheta}+\gamma_2^{\vartheta}$, $A_2=\mu^{\vartheta}+\alpha_1^{\vartheta}+\theta_1^{\vartheta}+\sigma^{\vartheta}$, $A_3=\mu^{\vartheta}+\alpha_2^{\vartheta}+\theta_2^{\vartheta}+\delta_1^{\vartheta}+\delta_2^{\vartheta}$, $A_4=\mu^{\vartheta}+\alpha_3^{\vartheta}+\theta_3^{\vartheta}+\delta_3^{\vartheta}+\delta_4^{\vartheta}$.

The definitions required for the existence and uniqueness are given as follows:

Definition 5. Let $C^*[0,\tau^*]$ be the class of continuous column vector $X(t)$ whose components $S,E,I,O,R,K,H\in C^*[0,\tau^*]$ are the class of continuous functions on the interval $[0,\tau^*]$. The norm of $X\in C^*[0,\tau^*]$ is given by

$$\|X\|=\sup_t\mid e^{-Nt}S(t)\mid+\sup_t\mid e^{-Nt}E(t)\mid+\sup_t\mid e^{-Nt}I(t)\mid+\sup_t\mid e^{-Nt}O(t)\mid+\sup_t\mid e^{-Nt}R(t)\mid+\sup_t\mid e^{-Nt}K(t)\mid+\sup_t\mid e^{-Nt}H(t)\mid,$$

where N is a natural number and when $t>\delta\geq m$, we write $C_{\delta}^*[0,\tau^*]$ and $C_{\delta}[0,\tau^*]$.

Definition 6. $X\in C^*[0,\tau^*]$ is a solution of IVP (6) if

(1) $(t,X(t))\in\mathcal{D}, t\in[0,\tau^*]$ where $\mathcal{D}=[0,\tau^*]\times\mathcal{K}$,
$\mathcal{K}=\{(S,E,I,O,R,K,H)\in\mathcal{R}_+^7:|S|\leq p,\ |E|\leq r,\ |I|\leq w,\ |O|\leq q\ |R|\leq l,\ |K|\leq m,\ |H|\leq h\}$,
$p,r,w,q,l,m,h\in R_+$ are constants.
(2) X(t) satisfies (6).

Theorem 2. *The IVP (6) has a unique solution $X\in C^*[0,\tau^*]$.*

Proof. From the properties of fractional calculus, Eq. (6) can be written as

$$I^{1-\vartheta}\frac{d}{dt}X(t)=B_1X(t)+S(t)B_2X(t)+E(t)B_3X(t)+I(t)B_4X(t)+O(t)B_5X(t)+\phi.$$

Operating by I^{ϑ} we obtain

$$X(t)=X(0)+I^{\vartheta}(B_1X(t)+S(t)B_2X(t)+E(t)B_3X(t)+I(t)B_4X(t)+O(t)B_5X(t)+\phi).\tag{7}$$

Now let $F:C^*[0,\tau^*]\to C^*[0,\tau^*]$ defined by

$$FX(t)=X(0)+I^{\vartheta}(B_1X(t)+S(t)B_2X(t)+E(t)B_3X(t)+I(t)B_4X(t)+O(t)B_5X(t)+\phi).\tag{8}$$

Then

$$e^{-Nt}(FX-FY)=e^{-Nt}I^{\vartheta}(B_1(X(t)-Y(t))+S(t)B_2(X(t)-Y(t))+E(t)B_3(X(t)-Y(t))+I(t)B_4(X(t)-Y(t))+O(t)B_5(X(t)-Y(t))).$$

$$e^{-Nt}(FX-FY) \le \left|\frac{1}{\Gamma(\vartheta)}\int_0^t (t-s)^{\vartheta-1}e^{-N(t-s)}\ e^{-Ns}\ (X(s)-Y(s))\ ds\right|\ (B_1+pB_2+rB_3+wB_4+qB_5)$$

$$\le (B_1+pB_2+rB_3+wB_4+qB_5)|\frac{1}{\Gamma(\vartheta)}\int_0^t (u)^{\vartheta-1}e^{-N(u)}|\|X-Y\|$$

$$\le \frac{(B_1+pB_2+rB_3+wB_4+qB_5)|\gamma(\vartheta,Nt)/\Gamma(\vartheta)|}{N^{\vartheta}}\|X-Y\|,$$

where $\gamma(\vartheta,Nt)$ is the lower incomplete gamma function and $u=t-s$. Since N is an arbitrary, we assume that $N^{\vartheta} \ge |\gamma(\vartheta,Nt)/\Gamma(\vartheta)|\ B_1+pB_2+rB_3+wB_4+qB_5$, then we get $\|FX-FY\| \le \|X-Y\|$. Operator F in (8) has a fixed point. Thus (7) has a unique solution $X \in C^*[0,\tau^*]$. From (7) we have

$$X(t) = X(0)+\frac{t^{\vartheta}}{\Gamma(\vartheta+1)}(B_1X(0)+S(0)B_2X(0)+E(0)B_3X(0)+I(0)B_4X(0)+O(0)B_5X(0)+\phi)+I^{\vartheta+1}(B_1X'(t)+S'(t)B_2X(t)$$
$$+S(t)B_2X'(t)+E'(t)B_3X(t)+E(t)B_3X'(t)+I'(t)B_4X(t)+I(t)B_4X'(t)+O'(t)B_5X(t)+O(t)B_5X'(t)).$$

$$e^{-Nt}X' = e^{-Nt}\frac{t^{\vartheta}}{\Gamma(\vartheta)}(B_1X(0)+S(0)B_2X(0)+E(0)B_3X(0)+I(0)B_4X(0)+O(0)B_5X(0)+\phi)+I^{\vartheta}(B_1X'(t)+S'(t)B_2X(t)$$
$$+S(t)B_2X'(t)+E'(t)B_3X(t)+E(t)B_3X'(t)+I'(t)B_4X(t)+I(t)B_4X'(t)+O'(t)B_5X(t)+O(t)B_5X'(t)).$$

Assuming that $X' \in C_{\sigma}^*[0,\tau^*]$. From (7) we get

$$\frac{dX}{dt} = \frac{d}{dt}I^{\vartheta}(B_1X(t)+S(t)B_2X(t)+E(t)B_3X(t)+I(t)B_4X(t)+O(t)B_5X(t)+\phi).$$

Operating by $I^{1-\vartheta}$ we get

$$I^{1-\vartheta}\frac{dX}{dt} = I^{1-\vartheta}\frac{d}{dt}I^{\vartheta}(B_1X(t)+S(t)B_2X(t)+E(t)B_3X(t)+I(t)B_4X(t)+O(t)B_5X(t)+\phi).$$

$${}_0^C D_t^{\vartheta}X(t) = B_1X(t)+S(t)B_2X(t)+E(t)B_3X(t)+I(t)B_4X(t)+O(t)B_5X(t)+\phi),$$

and

$$X(0) = X_0+I^{\vartheta}(B_1X(t)+S(t)B_2X(t)+E(t)B_3X(t)+I(t)B_4X(t)+O(t)B_5X(t)+\phi).$$

Therefore, Eq. (7) is equivalent to IVP (6). □

5. Equilibria and their stabilities

To calculate the equilibrium points, system (5) is written as:

$$\begin{aligned}
\Lambda^{\vartheta}-\left(\mu^{\vartheta}+\gamma_1^{\vartheta}+\gamma_2^{\vartheta}\right)S-\beta_1^{\vartheta}\frac{SE}{N}-\beta_2^{\vartheta}\frac{SI}{N}-\beta_3^{\vartheta}\frac{SO}{N}&=0,\\
\beta_1^{\vartheta}\left(1-\varepsilon_1^{\vartheta}-\varepsilon_2^{\vartheta}\right)\frac{SE}{N}-\left(\mu^{\vartheta}+\alpha_1^{\vartheta}+\theta_1^{\vartheta}+\sigma^{\vartheta}\right)E&=0,\\
\beta_1^{\vartheta}\varepsilon_1^{\vartheta}\frac{SE}{N}+\beta_2^{\vartheta}\frac{SI}{N}+\alpha_1^{\vartheta}E-\left(\mu^{\vartheta}+\alpha_2^{\vartheta}+\theta_2{}^{\vartheta}+\delta_1^{\vartheta}+\delta_2^{\vartheta}\right)I&=0,\\
\beta_1^{\vartheta}\varepsilon_2^{\vartheta}\frac{SE}{N}+\beta_3^{\vartheta}\frac{SO}{N}+\sigma^{\vartheta}E-\left(\mu^{\vartheta}+\alpha_3^{\vartheta}+\theta_3{}^{\vartheta}+\delta_3^{\vartheta}+\delta_4^{\vartheta}\right)O&=0,\\
\alpha_2^{\vartheta}I+\alpha_3^{\vartheta}O-\gamma_3^{\vartheta}R-\mu^{\vartheta}R&=0,\\
(1-\tau^{\vartheta})\gamma_1^{\vartheta}S+\theta_1^{\vartheta}E+\theta_2^{\vartheta}I+\theta_3^{\vartheta}O-\mu^{\vartheta}K&=0,\\
(\gamma_2^{\vartheta}+\tau^{\vartheta}\gamma_1^{\vartheta})S+\delta_2^{\vartheta}I+\delta_4^{\vartheta}O+\gamma_3^{\vartheta}R-(\mu_2^{\vartheta}+\mu^{\vartheta})H&=0.
\end{aligned} \tag{9}$$

After simplifications, we obtain the disease-free equilibrium point $\overline{DFE}=\left(\bar{S},0,0,0,\bar{K},\bar{H}\right)$, where $\bar{S}=\frac{\Lambda^{\vartheta}}{\mu^{\vartheta}+\gamma_1^{\vartheta}+\gamma_2^{\vartheta}}$, $\bar{K}=\frac{\left(1-\tau^{\vartheta}\right)\gamma_1^{\vartheta}\Lambda^{\vartheta}}{\mu^{\vartheta}\left(\mu^{\vartheta}+\gamma_1^{\vartheta}+\gamma_2^{\vartheta}\right)}$, $\bar{H}=\frac{\Lambda^{\vartheta}\left(\gamma_2^{\vartheta}+\gamma_1^{\vartheta}\tau^{\vartheta}\right)}{\left(\mu^{\vartheta}+\gamma_1^{\vartheta}+\gamma_2^{\vartheta}\right)\left(\mu_2^{\vartheta}+\mu^{\vartheta}\right)}$, and endemic equilibrium point $\widehat{EE}=(S^*,E^*,I^*,O^*,R^*,K^*,H^*)$, in which

$$S^*=\frac{N\left(\alpha_1^{\vartheta}+\theta_1^{\vartheta}+\mu^{\vartheta}+\sigma^{\vartheta}\right)}{\beta_1^{\vartheta}(1-\varepsilon_1^{\vartheta}-\varepsilon_2^{\vartheta})},$$

$$E^* = -\frac{\left(\Lambda^{\vartheta} - \frac{Ne_1\left(\mu^{\vartheta}+\gamma_1^{\vartheta}+\gamma_2^{\vartheta}\right)}{e_2\beta_1^{\vartheta}}\right)e_4e_3}{\frac{e_1\beta_3^{\vartheta}\left(\sigma^{\vartheta}+\frac{e_1\varepsilon_2^{\vartheta}}{e_2}\right)e_4}{e_2\beta_1^{\vartheta}} - \left(-\frac{e_1\beta_2^{\vartheta}\left(\alpha_1^{\vartheta}+\frac{e_1\varepsilon_1^{\vartheta}}{e_2}\right)}{e_2\beta_1^{\vartheta}} + \frac{e_1e_4}{e_2}\right)e_3},$$

$$I^* = \frac{e_2\beta_1^{\vartheta}\left(\Lambda^{\vartheta} - \frac{Ne_1\left(\mu^{\vartheta}+\gamma_1^{\vartheta}+\gamma_2^{\vartheta}\right)}{e_2\beta_1^{\vartheta}}\right)}{e_1\beta_2^{\vartheta}} - \frac{\beta_3^{\vartheta}\left(\Lambda^{\vartheta} - \frac{Ne_1\left(\mu^{\vartheta}+\gamma_1^{\vartheta}+\gamma_2^{\vartheta}\right)}{e_2\beta_1^{\vartheta}}\right)\left(\sigma^{\vartheta} + \frac{e_1\varepsilon_2^{\vartheta}}{e_2}\right)e_4}{\beta_2^{\vartheta}\left(\frac{e_1\beta_3^{\vartheta}\left(\sigma^{\vartheta}+\frac{e_1\varepsilon_2^{\vartheta}}{e_2}\right)e_4}{e_2\beta_1^{\vartheta}} - \left(-\frac{e_1\beta_2^{\vartheta}\left(\alpha_1^{\vartheta}+\frac{e_1\varepsilon_1^{\vartheta}}{e_2}\right)}{e_2\beta_1^{\vartheta}} + \frac{e_1e_4}{e_2}\right)e_3\right)}$$
$$+ \frac{\beta_1^{\vartheta}\left(\Lambda^{\vartheta} - \frac{Ne_1\left(\mu^{\vartheta}+\gamma_1^{\vartheta}+\gamma_2^{\vartheta}\right)}{e_2\beta_1^{\vartheta}}\right)e_4e_3}{\beta_2^{\vartheta}\left(\frac{e_1\beta_3^{\vartheta}\left(\sigma^{\vartheta}+\frac{e_1\varepsilon_2^{\vartheta}}{e_2}\right)e_4}{e_2\beta_1^{\vartheta}} - \left(-\frac{e_1\beta_2^{\vartheta}\left(\alpha_1^{\vartheta}+\frac{e_1\varepsilon_1^{\vartheta}}{e_2}\right)}{e_2\beta_1^{\vartheta}} + \frac{e_1e_4}{e_2}\right)e_3\right)},$$

$$O^* = \frac{\left(\Lambda^{\vartheta} - \frac{Ne_1\left(\mu^{\vartheta}+\gamma_1^{\vartheta}+\gamma_2^{\vartheta}\right)}{e_2\beta_1^{\vartheta}}\right)\left(\sigma^{\vartheta} + \frac{e_1\varepsilon_2^{\vartheta}}{e_2}\right)e_4}{\frac{e_1\beta_3^{\vartheta}\left(\sigma^{\vartheta}+\frac{e_1\varepsilon_2^{\vartheta}}{e_2}\right)e_4}{e_2\beta_1^{\vartheta}} - \left(-\frac{e_1\beta_2^{\vartheta}\left(\alpha_1^{\vartheta}+\frac{e_1\varepsilon_1^{\vartheta}}{e_2}\right)}{e_2\beta_1^{\vartheta}} + \frac{e_1e_4}{e_2}\right)e_3},$$

$$R^* = \frac{\alpha_3^{\vartheta}\left(\Lambda^{\vartheta} - \frac{Ne_1\left(\mu^{\vartheta}+\gamma_1^{\vartheta}+\gamma_2^{\vartheta}\right)}{e_2\beta_1^{\vartheta}}\right)\left(\sigma^{\vartheta} + \frac{e_1\varepsilon_2^{\vartheta}}{e_2}\right)e_4}{\left(\mu^{\vartheta}+\gamma_3^{\vartheta}\right)\left(\frac{e_1\beta_3^{\vartheta}\left(\sigma^{\vartheta}+\frac{e_1\varepsilon_2^{\vartheta}}{e_2}\right)e_4}{e_2\beta_1^{\vartheta}} - \left(-\frac{e_1\beta_2^{\vartheta}\left(\alpha_1^{\vartheta}+\frac{e_1\varepsilon_1^{\vartheta}}{e_2}\right)}{e_2\beta_1^{\vartheta}} + \frac{e_1e_4}{e_2}\right)e_3\right)} - \frac{\alpha_2^{\vartheta}}{\mu^{\vartheta}+\gamma_3^{\vartheta}}$$
$$\times\left(-\frac{e_2\beta_1^{\vartheta}\left(\Lambda^{\vartheta} - \frac{Ne_1\left(\mu^{\vartheta}+\gamma_1^{\vartheta}+\gamma_2^{\vartheta}\right)}{e_2\beta_1^{\vartheta}}\right)}{e_1\beta_2^{\vartheta}} + \frac{\beta_3^{\vartheta}\left(\Lambda^{\vartheta} - \frac{Ne_1\left(\mu^{\vartheta}+\gamma_1^{\vartheta}+\gamma_2^{\vartheta}\right)}{e_2\beta_1^{\vartheta}}\right)\left(\sigma^{\vartheta} + \frac{e_1\varepsilon_2^{\vartheta}}{e_2}\right)e_4}{\beta_2^{\vartheta}\left(\frac{e_1\beta_3^{\vartheta}\left(\sigma^{\vartheta}+\frac{e_1\varepsilon_2^{\vartheta}}{e_2}\right)e_4}{e_2\beta_1^{\vartheta}} - \left(-\frac{e_1\beta_2^{\vartheta}\left(\alpha_1^{\vartheta}+\frac{e_1\varepsilon_1^{\vartheta}}{e_2}\right)}{e_2\beta_1^{\vartheta}} + \frac{e_1e_4}{e_2}\right)e_3\right)}\right)$$
$$\times\left(-\frac{\beta_1^{\vartheta}\left(\Lambda^{\vartheta} - \frac{Ne_1\left(\mu^{\vartheta}+\gamma_1^{\vartheta}+\gamma_2^{\vartheta}\right)}{e_2\beta_1^{\vartheta}}\right)e_4e_3}{\beta_2^{\vartheta}\left(\frac{e_1\beta_3^{\vartheta}\left(\sigma^{\vartheta}+\frac{e_1\varepsilon_2^{\vartheta}}{e_2}\right)e_4}{e_2\beta_1^{\vartheta}} - \left(-\frac{e_1\beta_2^{\vartheta}\left(\alpha_1^{\vartheta}+\frac{e_1\varepsilon_1^{\vartheta}}{e_2}\right)}{e_2\beta_1^{\vartheta}} + \frac{e_1e_4}{e_2}\right)e_3\right)}\right),$$

$$K^* = \frac{N(1-\tau)e_1\gamma_1^{\vartheta}}{\mu^{\vartheta}e_2\beta_1^{\vartheta}} - \frac{\theta_2^{\vartheta}}{\mu^{\vartheta}}\left(-\frac{e_2\beta_1^{\vartheta}\left(\Lambda^{\vartheta} - \frac{Ne_1\left(\mu^{\vartheta}+\gamma_1^{\vartheta}+\gamma_2^{\vartheta}\right)}{e_2\beta_1^{\vartheta}}\right)}{e_1\beta_2^{\vartheta}} + \frac{\beta_3^{\vartheta}\left(\Lambda^{\vartheta} - \frac{Ne_1\left(\mu^{\vartheta}+\gamma_1^{\vartheta}+\gamma_2^{\vartheta}\right)}{e_2\beta_1^{\vartheta}}\right)\left(\sigma^{\vartheta} + \frac{e_1\varepsilon_2^{\vartheta}}{e_2}\right)e_4}{\beta_2^{\vartheta}\left(\frac{e_1\beta_3^{\vartheta}\left(\sigma^{\vartheta}+\frac{e_1\varepsilon_2^{\vartheta}}{e_2}\right)e_4}{e_2\beta_1^{\vartheta}} - \left(-\frac{e_1\beta_2^{\vartheta}\left(\alpha_1^{\vartheta}+\frac{e_1\varepsilon_1^{\vartheta}}{e_2}\right)}{e_2\beta_1^{\vartheta}} + \frac{e_1e_4}{e_2}\right)e_3\right)}\right)$$
$$+\frac{\theta_2^{\vartheta}}{\mu^{\vartheta}}\left(\frac{\beta_1^{\vartheta}\left(\Lambda^{\vartheta} - \frac{Ne_1\left(\mu^{\vartheta}+\gamma_1^{\vartheta}+\gamma_2^{\vartheta}\right)}{e_2\beta_1^{\vartheta}}\right)e_4e_3}{\beta_2^{\vartheta}\left(\frac{e_1\beta_3^{\vartheta}\left(\sigma^{\vartheta}+\frac{e_1\varepsilon_2^{\vartheta}}{e_2}\right)e_4}{e_2\beta_1^{\vartheta}} - \left(-\frac{e_1\beta_2^{\vartheta}\left(\alpha_1^{\vartheta}+\frac{e_1\varepsilon_1^{\vartheta}}{e_2}\right)}{e_2\beta_1^{\vartheta}} + \frac{e_1e_4}{e_2}\right)e_3\right)}\right)$$
$$-\frac{\left(\Lambda^{\vartheta} - \frac{Ne_1\left(\mu^{\vartheta}+\gamma_1^{\vartheta}+\gamma_2^{\vartheta}\right)}{e_2\beta_1^{\vartheta}}\right)\theta_1^{\vartheta}e_4e_3}{\mu^{\vartheta}\left(\frac{e_1\beta_3^{\vartheta}\left(\sigma^{\vartheta}+\frac{e_1\varepsilon_2^{\vartheta}}{e_2}\right)e_4}{e_2\beta_1^{\vartheta}} - \left(-\frac{e_1\beta_2^{\vartheta}\left(\alpha_1^{\vartheta}+\frac{e_1\varepsilon_1^{\vartheta}}{e_2}\right)}{e_2\beta_1^{\vartheta}} + \frac{e_1e_4}{e_2}\right)e_3\right)} + \frac{\left(\Lambda^{\vartheta} - \frac{Ne_1\left(\mu^{\vartheta}+\gamma_1^{\vartheta}+\gamma_2^{\vartheta}\right)}{e_2\beta_1^{\vartheta}}\right)\left(\sigma^{\vartheta} + \frac{e_1\varepsilon_2^{\vartheta}}{e_2}\right)e_4\theta_3^{\vartheta}}{\mu^{\vartheta}\left(\frac{e_1\beta_3^{\vartheta}\left(\sigma^{\vartheta}+\frac{e_1\varepsilon_2^{\vartheta}}{e_2}\right)e_4}{e_2\beta_1^{\vartheta}} - \left(-\frac{e_1\beta_2^{\vartheta}\left(\alpha_1^{\vartheta}+\frac{e_1\varepsilon_1^{\vartheta}}{e_2}\right)}{e_2\beta_1^{\vartheta}} + \frac{e_1e_4}{e_2}\right)e_3\right)},$$

$$H^{*}=\frac{Ne_1\left(\tau\gamma_1^{\vartheta}+\gamma_2^{\vartheta}\right)}{e_2\beta_1^{\vartheta}\left(\mu^{\vartheta}+\mu_2^{\vartheta}\right)}-\frac{\gamma_3^{\vartheta}}{\mu^{\vartheta}+\mu_2^{\vartheta}}\left(\frac{\alpha_3^{\vartheta}\left(\Lambda^{\vartheta}-\frac{Ne_1\left(\mu^{\vartheta}+\gamma_1^{\vartheta}+\gamma_2^{\vartheta}\right)}{e_2\beta_1^{\vartheta}}\right)\left(\sigma^{\vartheta}+\frac{e_1\varepsilon_2^{\vartheta}}{e_2}\right)e_4}{\left(-\mu^{\vartheta}-\gamma_3^{\vartheta}\right)\left(\frac{e_1\beta_3^{\vartheta}\left(\sigma^{\vartheta}+\frac{e_1\varepsilon_2^{\vartheta}}{e_2}\right)e_4}{e_2\beta_1^{\vartheta}}-\left(-\frac{e_1\beta_2^{\vartheta}\left(\alpha_1^{\vartheta}+\frac{e_1\varepsilon_1^{\vartheta}}{e_2}\right)}{e_2\beta_1^{\vartheta}}+\frac{e_1e_4}{e_2}\right)e_3\right)}\right)$$

$$-\frac{\gamma_3^{\vartheta}}{\mu^{\vartheta}+\mu_2^{\vartheta}}\frac{\alpha_2^{\vartheta}}{\mu^{\vartheta}+\gamma_3^{\vartheta}}\left(-\frac{e_2\beta_1^{\vartheta}\left(\Lambda^{\vartheta}-\frac{Ne_1\left(\mu^{\vartheta}+\gamma_1^{\vartheta}+\gamma_2^{\vartheta}\right)}{e_2\beta_1^{\vartheta}}\right)}{e_1\beta_2^{\vartheta}}+\frac{\beta_3^{\vartheta}\left(\Lambda^{\vartheta}-\frac{Ne_1\left(\mu^{\vartheta}+\gamma_1^{\vartheta}+\gamma_2^{\vartheta}\right)}{e_2\beta_1^{\vartheta}}\right)\left(\sigma^{\vartheta}+\frac{e_1\varepsilon_2^{\vartheta}}{e_2}\right)e_4}{\beta_2^{\vartheta}\left(\frac{e_1\beta_3^{\vartheta}\left(\sigma^{\vartheta}+\frac{e_1\varepsilon_2^{\vartheta}}{e_2}\right)e_4}{e_2\beta_1^{\vartheta}}-\left(-\frac{e_1\beta_2^{\vartheta}\left(\alpha_1^{\vartheta}+\frac{e_1\varepsilon_1^{\vartheta}}{e_2}\right)}{e_2\beta_1^{\vartheta}}+\frac{e_1e_4}{e_2}\right)e_3\right)}\right)$$

$$+\frac{\gamma_3^{\vartheta}}{\mu^{\vartheta}+\mu_2^{\vartheta}}\frac{\alpha_2^{\vartheta}}{\mu^{\vartheta}+\gamma_3^{\vartheta}}\frac{\beta_1^{\vartheta}\left(\Lambda^{\vartheta}-\frac{Ne_1\left(\mu^{\vartheta}+\gamma_1^{\vartheta}+\gamma_2^{\vartheta}\right)}{e_2\beta_1^{\vartheta}}\right)e_4e_3}{\beta_2^{\vartheta}\left(\frac{e_1\beta_3^{\vartheta}\left(\sigma^{\vartheta}+\frac{e_1\varepsilon_2^{\vartheta}}{e_2}\right)e_4}{e_2\beta_1^{\vartheta}}-\left(-\frac{e_1\beta_2^{\vartheta}\left(\alpha_1^{\vartheta}+\frac{e_1\varepsilon_1^{\vartheta}}{e_2}\right)}{e_2\beta_1^{\vartheta}}+\frac{e_1e_4}{e_2}\right)e_3\right)}$$

$$+\frac{\gamma_3^{\vartheta}}{\mu^{\vartheta}+\mu_2^{\vartheta}}\frac{\alpha_2^{\vartheta}}{\mu^{\vartheta}+\gamma_3^{\vartheta}}\frac{\left(\Lambda^{\vartheta}-\frac{Ne_1\left(\mu^{\vartheta}+\gamma_1^{\vartheta}+\gamma_2^{\vartheta}\right)}{e_2\beta_1^{\vartheta}}\right)\delta_4^{\vartheta}\left(\sigma^{\vartheta}+\frac{e_1\varepsilon_2^{\vartheta}}{e_2}\right)e_4}{\left(\frac{e_1\beta_3^{\vartheta}\left(\sigma^{\vartheta}+\frac{e_1\varepsilon_2^{\vartheta}}{e_2}\right)e_4}{e_2\beta_1^{\vartheta}}-\left(-\frac{e_1\beta_2^{\vartheta}\left(\alpha_1^{\vartheta}+\frac{e_1\varepsilon_1^{\vartheta}}{e_2}\right)}{e_2\beta_1^{\vartheta}}+\frac{e_1e_4}{e_2}\right)e_3\right)\left(-\mu^{\vartheta}-\mu_2^{\vartheta}\right)}$$

$$-\frac{\gamma_3^{\vartheta}\delta_2^{\vartheta}}{(\mu^{\vartheta}+\mu_2^{\vartheta})^2}\frac{\alpha_2^{\vartheta}}{\mu^{\vartheta}+\gamma_3^{\vartheta}}\left(-\frac{e_2\beta_1^{\vartheta}\left(\Lambda^{\vartheta}-\frac{Ne_1\left(\mu^{\vartheta}+\gamma_1^{\vartheta}+\gamma_2^{\vartheta}\right)}{e_2\beta_1^{\vartheta}}\right)}{e_1\beta_2^{\vartheta}}+\frac{\beta_3^{\vartheta}\left(\Lambda^{\vartheta}-\frac{Ne_1\left(\mu^{\vartheta}+\gamma_1^{\vartheta}+\gamma_2^{\vartheta}\right)}{e_2\beta_1^{\vartheta}}\right)\left(\sigma^{\vartheta}+\frac{e_1\varepsilon_2^{\vartheta}}{e_2}\right)e_4}{\beta_2^{\vartheta}\left(\frac{e_1\beta_3^{\vartheta}\left(\sigma^{\vartheta}+\frac{e_1\varepsilon_2^{\vartheta}}{e_2}\right)e_4}{e_2\beta_1^{\vartheta}}-\left(-\frac{e_1\beta_2^{\vartheta}\left(\alpha_1^{\vartheta}+\frac{e_1\varepsilon_1^{\vartheta}}{e_2}\right)}{e_2\beta_1^{\vartheta}}+\frac{e_1e_4}{e_2}\right)e_3\right)}\right)$$

$$+\frac{\gamma_3^{\vartheta}\delta_2^{\vartheta}}{(\mu^{\vartheta}+\mu_2^{\vartheta})^2}\frac{\alpha_2^{\vartheta}}{\mu^{\vartheta}+\gamma_3^{\vartheta}}\left(\frac{\beta_1^{\vartheta}\left(\Lambda^{\vartheta}-\frac{Ne_1\left(\mu^{\vartheta}+\gamma_1^{\vartheta}+\gamma_2^{\vartheta}\right)}{e_2\beta_1^{\vartheta}}\right)e_4e_3}{\beta_2^{\vartheta}\left(\frac{e_1\beta_3^{\vartheta}\left(\sigma^{\vartheta}+\frac{e_1\varepsilon_2^{\vartheta}}{e_2}\right)e_4}{e_2\beta_1^{\vartheta}}-\left(-\frac{e_1\beta_2^{\vartheta}\left(\alpha_1^{\vartheta}+\frac{e_1\varepsilon_1^{\vartheta}}{e_2}\right)}{e_2\beta_1^{\vartheta}}+\frac{e_1e_4}{e_2}\right)e_3\right)}\right),$$

where $e_1=\alpha_1^{\vartheta}+\theta_1^{\vartheta}+\mu^{\vartheta}+\sigma^{\vartheta}$, $e_2=1-\varepsilon_1^{\vartheta}-\varepsilon_2^{\vartheta}$,$e_3=-\alpha_3^{\vartheta}-\delta_3^{\vartheta}-\delta_4^{\vartheta}+\frac{\beta_3^{\vartheta}e_1}{\beta_1^{\vartheta}e_2}-\theta_3^{\vartheta}-\mu^{\vartheta}$, $e_4=-\alpha_2^{\vartheta}-\delta_1^{\vartheta}-\delta_2^{\vartheta}+\frac{\beta_2^{\vartheta}e_1}{\beta_1^{\vartheta}e_2}-\theta_2^{\vartheta}-\mu^{\vartheta}$.

5.1. Positivity and boundedness

In this subsection, we study the positivity and boundedness of the solution of model (5). Let $R_+^7=\zeta(t)\in R^7:\zeta(t)\geq 0$ and $\zeta(t)=[S(t),E(t),I(t),O(t),R(t),K(t),H(t)]^T$. Let us recall the following lemma, which we will use to prove the non-negativeness of the solution of model (5).

Lemma 1 (Generalized Mean Value Theorem)**.** *Assume that* $\omega(t)\in C[a,b]$ *and* ${}_0^C D_t^{\vartheta}\omega(t)\in C(a,b]$ *for* $0<\vartheta\leq 1$, *then* $\omega(t)=\omega(a)+\frac{1}{\Gamma(\vartheta)}{}_0^C D_t^{\vartheta}\omega(\tau)(t-a)^{\vartheta}$, *where* $0\leq\tau\leq t,\forall t\in(a,b]$.

Remark 1. If $\omega\in C[0,b]$ and ${}_0^C D_t^{\vartheta}(\omega(t))\geq 0,\forall t\in(0,b]$, then the function $\omega(t)$ is non-increasing for all $t\in[0,b]$.

Theorem 3. *The solution of model (5) along with initial conditions is bounded in* R_+^7.

Proof. Noting that the non-negative region R_+^7, is positivity invariant. From system (5), we obtain

$$\begin{aligned}
{}_0^C D_t^{\vartheta}S|_{S=0}&=\Lambda^{\vartheta}\geq 0,\\
{}_0^C D_t^{\vartheta}E|_{E=0}&=0\geq 0,\\
{}_0^C D_t^{\vartheta}I|_{I=0}&=\beta_1^{\vartheta}\varepsilon_1^{\vartheta}\frac{SE}{N}+\alpha_1^{\vartheta}E\geq 0,\\
{}_0^C D_t^{\vartheta}O|_{O=0}&=\beta_1^{\vartheta}\varepsilon_2^{\vartheta}\frac{SE}{N}+\sigma^{\vartheta}E\geq 0,
\end{aligned}\tag{10}$$

$${}_0^C D_t^{\vartheta} R|_{R=0} = \alpha_2^{\vartheta} I + \alpha_3^{\vartheta} O \geq 0,$$

$${}_0^C D_t^{\vartheta} K|_{K=0} = (1-\tau^{\vartheta})\gamma_1^{\vartheta} S + \theta_1^{\vartheta} E + \theta_2^{\vartheta} I + \theta_3^{\vartheta} O \geq 0,$$

$${}_0^C D_t^{\vartheta} H|_{H=0} = (\gamma_2^{\vartheta} + \tau^{\vartheta}\gamma_1^{\vartheta})S + \delta_2^{\vartheta} I + \delta_4^{\vartheta} O + \gamma_3^{\vartheta} R \geq 0.$$

If $(S(0), E(0), I(0), O(0), R(0), K(0), H(0)) \in R_+^7$, then according to system (10) and Remark 1, the solution of model (5) cannot escape from the hyperplanes $S=0, E=0, I=0, O=0, R=0, K=0$ and $H=0$. This concludes that the area R_+^7 is a positive invariant set. □

Theorem 4. *The region* $\mathcal{P} = \{(S(t), E(t), I(t), O(t), R(t), K(t), H(t)) \in R_+^7, 0 < S(t) + E(t) + I(t) + O(t) + R(t) + K(t) + H(t) \leq \frac{\Lambda^{\vartheta}}{\mu^{\vartheta}}\}$ *is a positive invariant set for the system (5).*

Proof. From model (5) we get ${}_0^C D_t^{\vartheta} N(t) = \Lambda^{\vartheta} - \mu^{\vartheta}(S(t) + E(t) + I(t) + O(t) + R(t) + K(t) + H(t)) - \mu_2^{\vartheta} H(t) - \delta_1^{\vartheta} I(t) - \delta_2^{\vartheta} I(t)$.
This gives ${}_0^C D_t^{\vartheta} \leq \Lambda^{\vartheta} - \mu^{\vartheta} N(t)$, where $\mu^{\vartheta} \leq \mu_2^{\vartheta}$. By applying the LT to the previous equation, we get
$s^{\vartheta}\omega(N) - s^{\vartheta-1}\omega(0) \leq \frac{\Lambda^{\vartheta}}{s} - \mu^{\vartheta}\omega(N)$, which further gives $\omega(N) \leq \frac{s^{-1}\Lambda}{s^{\vartheta}+\omega} + \frac{s^{\vartheta-1}N(0)}{s^{\vartheta}+\mu^{\vartheta}}$.
From Definitions 3, 4, we deduce that if $(S_0, E_0, I_0, O_0, R_0, K_0, H_0) \in R_+^7$, then
$N(t) \leq \Lambda^{\vartheta} t^{\vartheta} E_{\vartheta,\vartheta+1}(-\mu^{\vartheta} t^{\vartheta}) + E_{\vartheta,1}(-\mu^{\vartheta} t^{\vartheta}) N(0) \leq \frac{\Lambda^{\vartheta}}{\mu^{\vartheta}}(t^{\vartheta}\mu^{\vartheta} E_{\vartheta,\vartheta+1}(-\mu^{\vartheta} t^{\vartheta})) + E_{\vartheta,1}(-\mu^{\vartheta} t^{\vartheta}) \leq \frac{\Lambda^{\vartheta}}{\mu^{\vartheta}} \frac{1}{\Gamma(1)} = \frac{\Lambda^{\vartheta}}{\mu^{\vartheta}}$.
This means that $N(t)$ (the sum of populations) is bounded, thus, $S(t), E(t), I(t), O(t), R(t), K(t)$ *and* $H(t)$, are bounded. □

5.2. Stability of the equilibria

Here, we explain the necessary conditions for the stability of equilibria.

Theorem 5. *The disease-free equilibrium* $\overline{DFE}$ *of the model (5) is locally asymptotically stable (LAS) if* $\mathcal{R}_0 < 1$ *and is unstable if* $\mathcal{R}_0 > 1$.

Proof. The Jacobian matrix for system (5) with respect to $\overline{DFE}$ as follows:

$$J(\overline{DFE}) = \begin{bmatrix} -\gamma_1^{\vartheta} - \gamma_2^{\vartheta} - \mu^{\vartheta} & \frac{-\bar{S}\beta_1^{\vartheta}}{N} & \frac{-\bar{S}\beta_2^{\vartheta}}{N} & \frac{-\bar{S}\beta_3^{\vartheta}}{N} & 0 & 0 & 0 \\ 0 & (R_{03}-1)M_1 & 0 & 0 & 0 & 0 & 0 \\ 0 & \alpha_1^{\vartheta} + \frac{\bar{S}\beta_1^{\vartheta}\varepsilon_1^{\vartheta}}{N} & (R_{01}-1)M_2 & 0 & 0 & 0 & 0 \\ 0 & \sigma^{\vartheta} + \frac{\bar{S}\beta_1^{\vartheta}\varepsilon_2^{\vartheta}}{N} & 0 & (R_{02}-1)M_3 & 0 & 0 & 0 \\ 0 & 0 & \alpha_2^{\vartheta} & \alpha_3^{\vartheta} & -\gamma_3^{\vartheta} - \mu^{\vartheta} & 0 & 0 \\ 1-\gamma_1^{\vartheta}\tau^{\vartheta} & \theta_1^{\vartheta} & \theta_2^{\vartheta} & \theta_3^{\vartheta} & 0 & -\mu^{\vartheta} & 0 \\ \gamma_2^{\vartheta} + \gamma_1^{\vartheta}\tau^{\vartheta} & 0 & \delta_2^{\vartheta} & \delta_4^{\vartheta} & \gamma_3^{\vartheta} & 0 & -\mu^{\vartheta} - \mu_2^{\vartheta} \end{bmatrix}, \text{ where } \bar{S} = \frac{\Lambda^{\vartheta}}{\mu^{\vartheta} + \gamma_1^{\vartheta} + \gamma_2^{\vartheta}}, M_1 =$$

$\alpha_1^{\vartheta} + \mu^{\vartheta} + \sigma^{\vartheta} + \theta_1^{\vartheta}$, $M_2 = \alpha_2^{\vartheta} + \delta_1^{\vartheta} + \delta_2^{\vartheta} + \mu^{\vartheta} + \theta_2^{\vartheta}$ and $M_3 = \alpha_3^{\vartheta} + \delta_3^{\vartheta} + \delta_4^{\vartheta} + \mu^{\vartheta} + \theta_3^{\vartheta}$. So, the disease-free equilibrium $\overline{DFE}$ is LAS if all the eigenvalues λ_i, $i = 1, 2, \ldots, 7$ of the matrix $J(\overline{DFE})$ satisfy the condition

$$\left|arg\left(eig(J(\overline{DFE}))\right)\right| = |arg(\lambda_i)| > \vartheta\frac{\pi}{2}, \quad i = 1, 2, \ldots, 7. \tag{11}$$

To evaluate these eigenvalues, we solve the following characteristic equation

$$\left|J\left(\overline{DFE}\right) - \lambda\hat{I}\right| = 0, \tag{12}$$

where $\hat{I}$ is the identity matrix and λ is the eigenvalue. Thus:

$$\begin{aligned} P(\lambda) = &-\left(\lambda + \mu^{\vartheta}\right)\left(\gamma_3^{\vartheta} + \lambda + \mu^{\vartheta}\right)\left(\lambda + \mu^{\vartheta} + \mu_2^{\vartheta}\right)\left(\gamma_1^{\vartheta} + \gamma_2^{\vartheta} + \lambda + \mu^{\vartheta}\right)\left(\alpha_1^{\vartheta} + \lambda + \mu^{\vartheta} + \sigma^{\vartheta} + \theta_1^{\vartheta} - R_{03}(\alpha_1^{\vartheta} + \mu^{\vartheta} + \sigma^{\vartheta} + \theta_1^{\vartheta})\right) \\ &\times \left(\alpha_2^{\vartheta} + \delta_1^{\vartheta} + \delta_2^{\vartheta} + \lambda + \mu^{\vartheta} + \theta_2^{\vartheta} - R_{01}(\alpha_2^{\vartheta} + \delta_1^{\vartheta} + \delta_2^{\vartheta} + \mu^{\vartheta} + \theta_2^{\vartheta})\right) \\ &\times \left(\alpha_3^{\vartheta} + \delta_3^{\vartheta} + \delta_4^{\vartheta} + \lambda + \mu^{\vartheta} + \theta_3^{\vartheta} - R_{02}(\alpha_3^{\vartheta} + \delta_3^{\vartheta} + \delta_4^{\vartheta} + \mu^{\vartheta} + \theta_3^{\vartheta})\right) = 0. \end{aligned}$$

Hence, when $\mathcal{R}_0 = \max[\mathcal{R}_{01}, \mathcal{R}_{02}, \mathcal{R}_{03}] < 1$ and all the eigenvalues of $P(\lambda) = 0$ are negative. Thus, the $\overline{DFE}$ point is LAS. In addition, when $\mathcal{R}_0 > 1$, then at least one of the eigenvalues of $P(\lambda) = 0$ is positive. So, it gives us if $\mathcal{R}_0 > 1$ the $\overline{DFE}$ is unstable. □

Theorem 6. *The endemic equilibrium* $\widehat{E\bar{E}}$ *of model (5) is LAS if* $\mathcal{R}_0 > 1$ *and unstable otherwise.*

Proof. The Jacobian matrix $J\left(\widehat{E\bar{E}}\right)$ is given by

$$J\left(\widehat{E\bar{E}}\right) = \begin{bmatrix} a_4 & \frac{-S^*\beta_1^{\vartheta}}{N} & \frac{-S^*\beta_2^{\vartheta}}{N} & \frac{-S^*\beta_3^{\vartheta}}{N} & 0 & 0 & 0 \\ a_5 & a_1(R_{03}-1) & 0 & 0 & 0 & 0 & 0 \\ a_6 & a_7 & a_2(R_{01}-1) & 0 & 0 & 0 & 0 \\ a_9 & a_8 & 0 & a_3(R_{02}-1) & 0 & 0 & 0 \\ 0 & 0 & a_2 & a_3 & -\gamma_3^{\vartheta} - \mu^{\vartheta} & 0 & 0 \\ a_{11} & \theta_1^{\vartheta} & \theta_2^{\vartheta} & \theta_3^{\vartheta} & 0 & -\mu^{\vartheta} & 0 \\ a_{10} & 0 & \delta_2^{\vartheta} & \delta_4^{\vartheta} & \gamma_3^{\vartheta} & 0 & -\mu^{\vartheta} - \mu_2^{\vartheta} \end{bmatrix},$$

where $a_1 = \alpha_1^{\vartheta} + \mu^{\vartheta} + \sigma^{\vartheta} + \theta_1^{\vartheta}$, $a_2 = \alpha_2^{\vartheta} + \mu^{\vartheta} + \delta_1^{\vartheta} + \delta_2^{\vartheta} + \theta_2^{\vartheta}$, $a_3 = \alpha_3^{\vartheta} + \mu^{\vartheta} + \delta_3^{\vartheta} + \delta_4^{\vartheta} + \theta_3^{\vartheta}$, $a_4 = -\gamma_1^{\vartheta} - \gamma_2^{\vartheta} - \mu^{\vartheta} - \frac{E^*\beta_1^{\vartheta}}{N} - \frac{I^*\beta_2^{\vartheta}}{N} - \frac{O^*\beta_3^{\vartheta}}{N}$, $a_5 = \frac{E^*\beta_1^{\vartheta}(1-\varepsilon_1^{\vartheta}-\varepsilon_2^{\vartheta})}{N}$, $a_6 = \frac{I^*\beta_2^{\vartheta} + E^*\beta_1^{\vartheta}\varepsilon_1^{\vartheta}}{N}$, $a_7 = \alpha_1^{\vartheta} + \frac{S^*\beta_1^{\vartheta}\varepsilon_1^{\vartheta}}{N}$, $a_8 = \sigma^{\vartheta} + \frac{S^*\beta_1^{\vartheta}\varepsilon_2^{\vartheta}}{N}$, $a_9 = \frac{O^*\beta_3^{\vartheta} + E^*\beta_1^{\vartheta}\varepsilon_2^{\vartheta}}{N}$, $a_{10} = \gamma_2^{\vartheta} + \gamma_1^{\vartheta}\tau^{\vartheta}$, $a_{11} = 1 - \gamma_1^{\vartheta}\tau^{\vartheta}$.

From the characteristic equation $|J(\widehat{EE}) - \lambda \hat{I}| = 0$, we get $P(\lambda) = -(\lambda + \mu^{\vartheta})(\gamma_3^{\vartheta} + \lambda + \mu^{\vartheta})(\lambda + \mu^{\vartheta} + \mu_2^{\vartheta})[\lambda^4 + \lambda^3 B_1 + \lambda^2 B_2 + \lambda^3 B_3 + B_4]$, where $B_1 = (a_1 + a_2)(1 - R_{03}) + a_3(1 - R_{02})$, $B_2 = a_1a_2(1 - R_{01} + R_{01}R_{03}) + a_1a_3(1 - R_{02} - R_{03} + R_{02}R_{03}) + a_2a_3(1 - R_{01} - R_{02}) - a_1a_4(1 - R_{03}) - a_1a_4(1 - R_{03}) - a_2a_4(1 - R_{01}) - a_3a_4(1 - R_{02}) + a_5S\beta_1 + a_6S\beta_2^{\vartheta} + a_9S\beta_3^{\vartheta}$, $B_3 = a_1a_2a_3(1 - R_{01} - R_{02} + R_{01}R_{02} - R_{03} + R_{01}R_{03} + R_{02}R_{03} - R_{01}R_{02}R_{03}) - a_1a_2a_4(1 - R_{01} - R_{03} + R_{01}R_{03}) - a_1a_3a_4(1 - R_{02} - R_{03} + R_{02}R_{03}) - a_2a_3a_4(1 - R_{01} - R_{02} + R_{01}R_{02}) + (a_2a_5S\beta_1^{\vartheta} + a_2a_9S\beta_3^{\vartheta})(1 - R_{01}) + (a_3a_5S\beta_1^{\vartheta} + a_3a_6S\beta_2^{\vartheta})(1 - R_{02}) + (a_1a_9S\beta_3^{\vartheta} + a_1a_6S\beta_2^{\vartheta})(1 - R_{03}) + a_5a_7S\beta_2^{\vartheta} + a_5a_8S\beta_3^{\vartheta}$, $B_4 = -a_1a_2a_3a_4(1 - R_{01} - R_{02} + R_{01}R_{02} - R_{03} + R_{01}R_{03} + R_{02}R_{03} + R_{01}R_{02}R_{03}) + a_2a_3a_5S\beta_1^{\vartheta}(1 - R_{01} - R_{02} + R_{01}R_{02}) + a_1a_3a_6S\beta_2^{\vartheta}(1 - R_{02} - R_{03} + R_{02}R_{03}) + a_3a_5a_7S\beta_2^{\vartheta}(1 - R_{02}) + a_2a_5a_8S\beta_3^{\vartheta}(1 - R_{01}) + a_1a_2a_9R_{01}R_{03}S\beta_3^{\vartheta}(1 - R_{01} - R_{03} + R_{01}R_{03})$.

According to Routh–Hurwitz criteria, if $B_1 > 0$, $B_3 > 0, B_4 > 0$, and $B_1B_2B_3 > {B_3}^2 + {B_1}^2B_4$ hold, $\widehat{EE}$ is locally asymptotically stable. □

5.3. Basic reproduction number

The basic reproduction number ("R_0") by using next generation matrix method (NGMM) [34,35], is computed for the local stability of the disease-free equilibrium. The disease transmission coefficient, or "R_0", indicates the extent of the virus spread, i.e. the number of people who can be infected with it. Biologically, if $\mathcal{R}_0 < 1$ then the disease will disappear, if $\mathcal{R}_0 > 1$, the infection exists in the population. To determine $\mathcal{R}_0$ which is considered as the spectral radius of the next generation matrix $\left(\mathbb{F}\mathbb{V}^{-1}\right)$, we write the compartments which are infected from the system (5) in corresponding rows of the $\mathcal{F}$ and write the right hand side of model (5) as $\mathcal{F} - \mathcal{V}$, where $\mathcal{F}$ is the transmission part, representing the production of new infection, and $\mathcal{V}$ is the transition part which expressing the change in state. Therefore,

$$\mathcal{F} = \begin{pmatrix} 0 \\ \beta_1^{\vartheta}(1 - \varepsilon_1^{\vartheta} - \varepsilon_2^{\vartheta})\frac{SE}{N} \\ \beta_2^{\vartheta}\frac{SI}{N} \\ \beta_3^{\vartheta}\frac{SO}{N} \\ 0 \\ 0 \\ 0 \end{pmatrix},$$

and

$$\mathcal{V} = \begin{pmatrix} \left(\mu^{\vartheta} + \gamma_1^{\vartheta} + \gamma_2^{\vartheta}\right)S + \beta_1^{\vartheta}\frac{SE}{N} + \beta_2^{\vartheta}\frac{SI}{N} + \beta_3^{\vartheta}\frac{SO}{N}\$\mu^{\vartheta} + \alpha_1^{\vartheta} + \theta_1^{\vartheta} + \sigma^{\vartheta})E \\ -\beta_1^{\vartheta}\varepsilon_1^{\vartheta}\frac{SE}{N} - \alpha_1^{\vartheta}E + \left(\mu^{\vartheta} + \alpha_2^{\vartheta} + \theta_2{}^{\vartheta} + \delta_1^{\vartheta} + \delta_2^{\vartheta}\right)I \\ -\beta_1^{\vartheta}\varepsilon_2^{\vartheta}\frac{SE}{N} - \sigma^{\vartheta}E + \left(\mu^{\vartheta} + \alpha_3^{\vartheta} + \theta_3{}^{\vartheta} + \delta_3^{\vartheta} + \delta_4^{\vartheta}\right)O \\ -\alpha_2^{\vartheta}I - \alpha_3^{\vartheta}O + \gamma_3^{\vartheta}R + \mu^{\vartheta}R \\ -(1 - \tau^{\vartheta})\gamma_1^{\vartheta}S - \theta_1^{\vartheta}E - \theta_2^{\vartheta}I - \theta_3^{\vartheta}O + \mu^{\vartheta}K \\ -(\gamma_2^{\vartheta} + \tau^{\vartheta}\gamma_1^{\vartheta})S - \delta_2^{\vartheta}I - \delta_4^{\vartheta}O - \gamma_3^{\vartheta}R + (\mu_2^{\vartheta} + \mu^{\vartheta})H \end{pmatrix}.$$

By using the next generation matrix method [34,35], the matrices $\mathbb{F}$ and $\mathbb{V}$ at $\overline{DFE}$ are obtained by $\mathbb{F} = \left[\frac{\partial \mathcal{F}_x(\overline{DFE})}{\partial t_y}\right]$ and $\mathbb{V} = \left[\frac{\partial\ \mathcal{V}_x(\overline{DFE})}{\partial t_y}\right]$, $1 \le x, y \le 3$. This implies,

$$\mathbb{F} = \begin{pmatrix} \beta_1^{\vartheta}\frac{S}{N}\left(1 - \varepsilon_1^{\vartheta} - \varepsilon_2^{\vartheta}\right) & 0 & 0 \\ 0 & \beta_2^{\vartheta}\frac{S}{N} & 0 \\ 0 & 0 & \beta_3^{\vartheta}\frac{S}{N} \end{pmatrix},$$

$$\mathbb{V} = \begin{pmatrix} \alpha_1^{\vartheta} + \mu^{\vartheta} + \sigma^{\vartheta} + \theta_1^{\vartheta} & 0 & 0 \\ -\alpha_1^{\vartheta} - \beta_1^{\vartheta}\varepsilon_1^{\vartheta}\frac{S}{N} & \delta_1^{\vartheta} + \delta_2^{\vartheta} + \mu^{\vartheta} + \theta_2^{\vartheta} + \alpha_2^{\vartheta} & 0 \\ -\sigma^{\vartheta} - \beta_1^{\vartheta}\varepsilon_2^{\vartheta}\frac{S}{N} & 0 & \alpha_3^{\vartheta} + \delta_3^{\vartheta} + \delta_4^{\vartheta} + \mu^{\vartheta} + \theta_3^{\vartheta} \end{pmatrix}.$$

The basic reproduction number ($\mathcal{R}_0$) of the disease is calculated with the help of the spectral radius of the matrix $\left(\mathbb{F}\mathbb{V}^{-1}\right)$ at the equilibrium point $\overline{DFE}$, which is indicated by three cases namely $\mathcal{R}_{01}$, $\mathcal{R}_{02}$ and $\mathcal{R}_{03}$:

$$\mathcal{R}_{01} = \frac{\Lambda^{\vartheta}\beta_2^{\vartheta}}{N\left(\gamma_1^{\vartheta} + \gamma_2^{\vartheta} + \mu^{\vartheta}\right)\left(\alpha_2^{\vartheta} + \delta_1^{\vartheta} + \delta_2^{\vartheta} + \mu^{\vartheta} + \theta_2^{\vartheta}\right)},$$

$$\mathcal{R}_{02} = \frac{\Lambda^{\vartheta}\beta_3^{\vartheta}}{N\left(\gamma_1^{\vartheta} + \gamma_2^{\vartheta} + \mu^{\vartheta}\right)\left(\delta_3^{\vartheta} + \alpha_3^{\vartheta} + \delta_4^{\vartheta} + \mu^{\vartheta} + \theta_3^{\vartheta}\right)},$$

$$\mathcal{R}_{03} = \frac{\Lambda^{\vartheta}\beta_1^{\vartheta}\left(1 - \varepsilon_1^{\vartheta} - \varepsilon_2^{\vartheta}\right)}{N\left(\gamma_1^{\vartheta} + \gamma_2^{\vartheta} + \mu^{\vartheta}\right)\left(\alpha_1^{\vartheta} + \mu^{\vartheta} + \sigma^{\vartheta} + \theta_1^{\vartheta}\right)},$$

in which

$$\mathcal{R}_0 = \max\left[\mathcal{R}_{01}, \mathcal{R}_{02}, \mathcal{R}_{03}\right]. \tag{13}$$

6. Sensitivity analysis

In this section, we analyze the sensitivity of $\mathcal{R}_{01}, \mathcal{R}_{02}$ and $\mathcal{R}_{03}$ according to parameters that affect the reproduction number. A sensitivity measure shows the relative changes that may occur in variables that change with a change in a given parameter. We have applied the same method as in [36]. Given the importance of the reproduction number in calculating disease prevalence, it is necessary to assess the sensitivities of the parameters with respect to $\mathcal{R}_0$. The fractional derivative for R_{01}, R_{02} and R_{03} is given by

$$\frac{\partial \mathcal{R}_{01}}{\partial \Lambda^{\vartheta}} = \frac{\beta_2^{\vartheta}}{N\left(\gamma_1^{\vartheta}+\gamma_2^{\vartheta}+\mu^{\vartheta}\right)(\alpha_2^{\vartheta}+\delta_1^{\vartheta}+\delta_2^{\vartheta}+\mu^{\vartheta}+\theta_2^{\vartheta})} > 0,$$

$$\frac{\partial \mathcal{R}_{02}}{\partial \Lambda^{\vartheta}} = \frac{\beta_3^{\vartheta}}{N\left(\gamma_1^{\vartheta}+\gamma_2^{\vartheta}+\mu^{\vartheta}\right)(\delta_3^{\vartheta}+\alpha_3^{\vartheta}+\delta_4^{\vartheta}+\mu^{\vartheta}+\theta_3^{\vartheta})} > 0,$$

$$\frac{\partial \mathcal{R}_{03}}{\partial \Lambda^{\vartheta}} = \frac{-\beta_1^{\vartheta}(\varepsilon_1^{\vartheta}+\varepsilon_2^{\vartheta}-1)}{N\left(\gamma_1^{\vartheta}+\gamma_2^{\vartheta}+\mu^{\vartheta}\right)(\alpha_1^{\vartheta}+\mu^{\vartheta}+\sigma^{\vartheta}+\theta_1^{\vartheta})} < 0,$$

$$\frac{\partial \mathcal{R}_{01}}{\partial \beta_2^{\vartheta}} = \frac{\Lambda^{\vartheta}}{N\left(\gamma_1^{\vartheta}+\gamma_2^{\vartheta}+\mu^{\vartheta}\right)(\alpha_2^{\vartheta}+\delta_1^{\vartheta}+\delta_2^{\vartheta}+\mu^{\vartheta}+\theta_2^{\vartheta})} > 0,$$

$$\frac{\partial \mathcal{R}_{02}}{\partial \beta_3^{\vartheta}} = \frac{\Lambda^{\vartheta}}{N\left(\gamma_1^{\vartheta}+\gamma_2^{\vartheta}+\mu^{\vartheta}\right)(\delta_3^{\vartheta}+\alpha_3^{\vartheta}+\delta_4^{\vartheta}+\mu^{\vartheta}+\theta_3^{\vartheta})} > 0,$$

$$\frac{\partial \mathcal{R}_{03}}{\partial \beta_1^{\vartheta}} = \frac{-\Lambda^{\vartheta}(\varepsilon_1^{\vartheta}+\varepsilon_2^{\vartheta}-1)}{N\left(\gamma_1^{\vartheta}+\gamma_2^{\vartheta}+\mu^{\vartheta}\right)(\alpha_1^{\vartheta}+\mu^{\vartheta}+\sigma^{\vartheta}+\theta_1^{\vartheta})} < 0,$$

$$\frac{\partial \mathcal{R}_{03}}{\partial \varepsilon_1^{\vartheta}} = \frac{\partial \mathcal{R}_{03}}{\partial \varepsilon_2^{\vartheta}} = \frac{-\Lambda^{\vartheta}\beta_1^{\vartheta}}{N\left(\gamma_1^{\vartheta}+\gamma_2^{\vartheta}+\mu^{\vartheta}\right)(\alpha_1^{\vartheta}+\mu^{\vartheta}+\sigma^{\vartheta}+\theta_1^{\vartheta})} < 0,$$

$$\frac{\partial \mathcal{R}_{01}}{\partial \gamma_1^{\vartheta}} = \frac{\partial \mathcal{R}_{01}}{\partial \gamma_2^{\vartheta}} = \frac{-\Lambda^{\vartheta}\beta_2^{\vartheta}}{N\left(\gamma_1^{\vartheta}+\gamma_2^{\vartheta}+\mu^{\vartheta}\right)^2(\alpha_2^{\vartheta}+\delta_1^{\vartheta}+\delta_2^{\vartheta}+\mu^{\vartheta}+\theta_2^{\vartheta})} < 0,$$

$$\frac{\partial \mathcal{R}_{02}}{\partial \gamma_1^{\vartheta}} = \frac{\partial \mathcal{R}_{02}}{\partial \gamma_2^{\vartheta}} = \frac{-\Lambda^{\vartheta}\beta_3^{\vartheta}}{N\left(\gamma_1^{\vartheta}+\gamma_2^{\vartheta}+\mu^{\vartheta}\right)^2(\delta_3^{\vartheta}+\alpha_3^{\vartheta}+\delta_4^{\vartheta}+\mu^{\vartheta}+\theta_3^{\vartheta})} < 0,$$

$$\frac{\partial \mathcal{R}_{03}}{\partial \gamma_1^{\vartheta}} = \frac{\partial \mathcal{R}_{03}}{\partial \gamma_2^{\vartheta}} = \frac{\Lambda^{\vartheta}\beta_1^{\vartheta}(\varepsilon_1^{\vartheta}+\varepsilon_2^{\vartheta}-1)}{N\left(\gamma_1^{\vartheta}+\gamma_2^{\vartheta}+\mu^{\vartheta}\right)^2(\alpha_1^{\vartheta}+\mu^{\vartheta}+\sigma^{\vartheta}+\theta_1^{\vartheta})} > 0,$$

$$\frac{\partial \mathcal{R}_{01}}{\partial \alpha_2{}^{\vartheta}} = \frac{\partial \mathcal{R}_{01}}{\partial \theta_2{}^{\vartheta}} = \frac{\partial \mathcal{R}_{01}}{\partial \delta_1{}^{\vartheta}} = \frac{\partial \mathcal{R}_{01}}{\partial \delta_2{}^{\vartheta}} = \frac{-\Lambda^{\vartheta}\beta_2{}^{\vartheta}}{N\left(\gamma_1{}^{\vartheta}+\gamma_2{}^{\vartheta}+\mu^{\vartheta}\right)(\alpha_2{}^{\vartheta}+\delta_1{}^{\vartheta}+\delta_2{}^{\vartheta}+\mu^{\vartheta}+\theta_2{}^{\vartheta})^2} < 0,$$

$$\frac{\partial \mathcal{R}_{02}}{\partial \alpha_3{}^{\vartheta}} = \frac{\partial \mathcal{R}_{02}}{\partial \theta_3{}^{\vartheta}} = \frac{\partial \mathcal{R}_{02}}{\partial \delta_3{}^{\vartheta}} = \frac{\partial \mathcal{R}_{02}}{\partial \delta_4{}^{\vartheta}} = \frac{-\Lambda^{\vartheta}\beta_3{}^{\vartheta}}{N\left(\gamma_1{}^{\vartheta}+\gamma_2{}^{\vartheta}+\mu^{\vartheta}\right)(\delta_3{}^{\vartheta}+\alpha_3{}^{\vartheta}+\delta_4{}^{\vartheta}+\mu^{\vartheta}+\theta_3{}^{\vartheta})^2} < 0,$$

$$\frac{\partial \mathcal{R}_{03}}{\partial \alpha_1{}^{\vartheta}} = \frac{\partial \mathcal{R}_{03}}{\partial \sigma^{\vartheta}} = \frac{\partial \mathcal{R}_{03}}{\partial \theta_2{}^{\vartheta}} = \frac{\Lambda^{\vartheta}\beta_1{}^{\vartheta}(\varepsilon_1{}^{\vartheta}+\varepsilon_2{}^{\vartheta}-1)}{N\left(\gamma_1{}^{\vartheta}+\gamma_2{}^{\vartheta}+\mu^{\vartheta}\right)(\alpha_1{}^{\vartheta}+\mu^{\vartheta}+\sigma^{\vartheta}+\theta_1{}^{\vartheta})^2} > 0,$$

$$\frac{\partial \mathcal{R}_{01}}{\partial \mu^{\vartheta}} = \frac{-\Lambda^{\vartheta}\beta_2{}^{\vartheta}}{N\left(\gamma_1{}^{\vartheta}+\gamma_2{}^{\vartheta}+\mu^{\vartheta}\right)(\alpha_2{}^{\vartheta}+\delta_1{}^{\vartheta}+\delta_2{}^{\vartheta}+\mu^{\vartheta}+\theta_2{}^{\vartheta})^2} - \frac{\Lambda^{\vartheta}\beta_2{}^{\vartheta}}{N\left(\gamma_1{}^{\vartheta}+\gamma_2{}^{\vartheta}+\mu^{\vartheta}\right)^2(\alpha_2{}^{\vartheta}+\delta_1{}^{\vartheta}+\delta_2{}^{\vartheta}+\mu^{\vartheta}+\theta_2{}^{\vartheta})} < 0,$$

$$\frac{\partial \mathcal{R}_{02}}{\partial \mu^{\vartheta}} = \frac{-\Lambda^{\vartheta}\beta_3{}^{\vartheta}}{N\left(\gamma_1{}^{\vartheta}+\gamma_2{}^{\vartheta}+\mu^{\vartheta}\right)(\delta_3{}^{\vartheta}+\alpha_3{}^{\vartheta}+\delta_4{}^{\vartheta}+\mu^{\vartheta}+\theta_3{}^{\vartheta})^2} - \frac{\Lambda^{\vartheta}\beta_3{}^{\vartheta}}{N\left(\gamma_1{}^{\vartheta}+\gamma_2{}^{\vartheta}+\mu^{\vartheta}\right)^2(\delta_3{}^{\vartheta}+\alpha_3{}^{\vartheta}+\delta_4{}^{\vartheta}+\mu^{\vartheta}+\theta_3{}^{\vartheta})} < 0,$$

$$\frac{\partial \mathcal{R}_{03}}{\partial \mu^{\vartheta}} = \frac{\Lambda^{\vartheta}\beta_1{}^{\vartheta}(\varepsilon_1{}^{\vartheta}+\varepsilon_2{}^{\vartheta}-1)}{N\left(\gamma_1{}^{\vartheta}+\gamma_2{}^{\vartheta}+\mu^{\vartheta}\right)(\alpha_1{}^{\vartheta}+\mu^{\vartheta}+\sigma^{\vartheta}+\theta_1{}^{\vartheta})^2} + \frac{\Lambda^{\vartheta}\beta_1{}^{\vartheta}(\varepsilon_1{}^{\vartheta}+\varepsilon_2{}^{\vartheta}-1)}{N\left(\gamma_1{}^{\vartheta}+\gamma_2{}^{\vartheta}+\mu^{\vartheta}\right)^2(\alpha_1{}^{\vartheta}+\mu^{\vartheta}+\sigma^{\vartheta}+\theta_1{}^{\vartheta})} > 0.$$

In the sensitivity analysis, it can be seen that $\mathcal{R}_{01}$ increases with parameters $\Lambda^{\vartheta}, \beta_2^{\vartheta}$ and decreases with $\gamma_1^{\vartheta}, \gamma_2^{\vartheta}, \alpha_2^{\vartheta}, \theta_2^{\vartheta}, \delta_1^{\vartheta}, \delta_2^{\vartheta}, \mu^{\vartheta}$. $\mathcal{R}_{02}$ increases with parameters $\Lambda^{\vartheta}, \beta_3^{\vartheta}$, and decreases with $\gamma_1^{\vartheta}, \gamma_2^{\vartheta}, \alpha_3^{\vartheta}, \theta_3^{\vartheta}, \delta_3^{\vartheta}, \delta_4^{\vartheta}, \mu^{\vartheta}$ and $\mathcal{R}_{03}$ decreases with parameters $\Lambda^{\vartheta}, \beta_1^{\vartheta}, \varepsilon_1^{\vartheta}, \varepsilon_2^{\vartheta}$, and increases with $\alpha_1^{\vartheta}, \gamma_1^{\vartheta}, \gamma_2^{\vartheta}, \sigma^{\vartheta}, \theta_2^{\vartheta}, \mu^{\vartheta}$. This situation explains that in order to decrease the outbreak of the disease, parameters with negative values of the fractional derivative in the population must be maximized.

7. Parameter estimation

The parameter estimation (PE) technique is a very useful method, which has been very popular recently, which allows us to find the closest parameter values to the real data, while obtaining the curve that best fits the real data. Thanks to PE method, the most realistic parameter values are calculated for the mathematical model created. In most of the studies in the literature, the numerical values of the parameters are the estimated parameter values used in the previous articles. This method increases the value of our study in terms of calculating model-specific parameter values. The PE technique is a very useful method in obtaining the most suitable curve for the real data, while providing the parameter values closest to the real values. The working principle of this method can be expressed by the following algorithm:

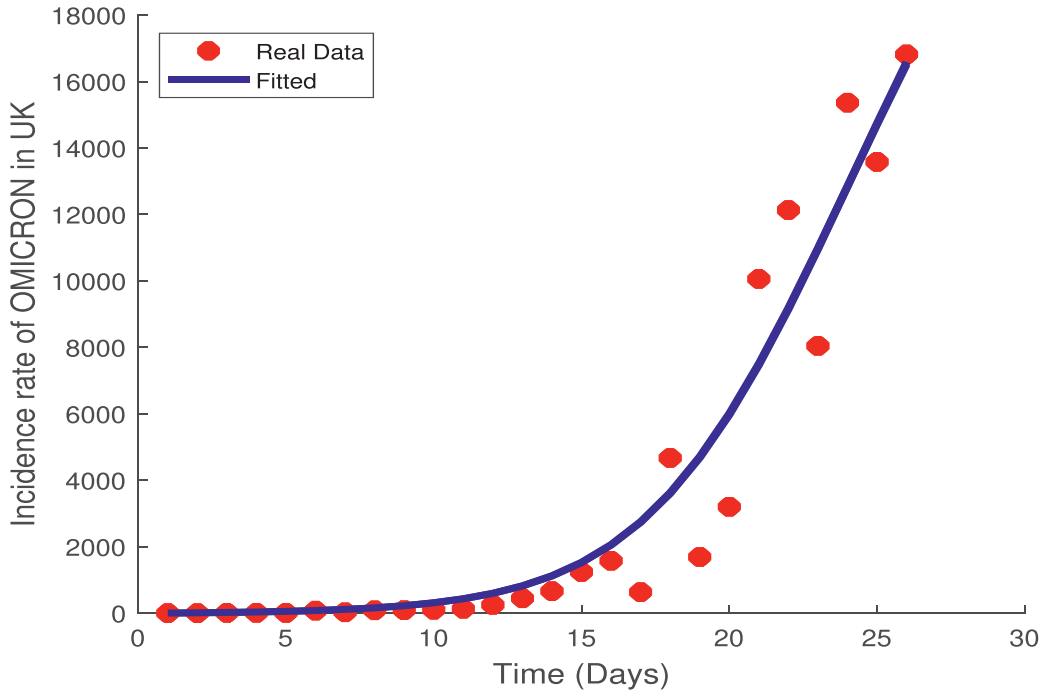

Fig. 1. Real cases of Omicron variant in the U.K. from November 28 to December 23, 2021 and the best-fit curve from the proposed model.

- Find coefficients c that solve the problem $\min_c \|X(c, cdata) - ydata\|_2^2 = \min_c \sum_i (X(c, cdata_i) - ydata_i)^2$, given input data $cdata$, and the observed output $ydata$, where $cdata$ and $ydata$ are matrices or vectors, and $X(c, cdata)$ is a matrix-valued or vector-valued function of the same size as $ydata$.
- If there are boundaries, then lower and upper bounds lb, and ub can be assigned, respectively. The arguments c, lb, and ub can be vectors or matrices.
- The MATLAB code *lsqcurvefit* simply provides a convenient interface for data-fitting problems and it requires the user-defined function to compute the following vector-valued function

$$X(c, cdata) = \begin{bmatrix} X(c, cdata(1)) \\ X(c, cdata(2)) \\ X(c, cdata(3)) \\ \vdots \\ X(c, cdata(k)) \end{bmatrix}.$$

There are a total of 23 parameter values in the model we constructed for interaction between COVID-19 and heart attack. We fit a total of 21 parameter values with the aim of the above algorithm by using real Omicron data in the UK (https://www.gov.uk), and we have calculated the Λ (recruitment rate) and μ (natural death rate) by using the current life expectancy for U.K. (81.65 years) and the total population of the U.K., 68,431,539 (https://www.macrotrends.net/countries/GBR/united-kingdom/life-expectancy). We covered the daily cases from November 28 to December 23. If the initial conditions are considered as U.K.'s total population and the initial exposed and quarantined individuals $E(0) = 55000, K(0) = 15000$, since $N(0) = S(0) + E(0) + I(0) + O(0) + R(0) + K(0) + H(0)$, $S(0) = 58162089$, $O(0) = 2$, $I(0) = 39565$, other remaining populations are calculated as $R(0) = 10152722$, $K(0) = 15000$, and $H(0) = 300$. Real Omicron cases are shown with blue filled circles in Fig. 1. The parameter values used in the modeling are given in Table 1 along with the best fitted values obtained by least squares curve fitting method (LCM). In addition, the second infectious rate $\mathcal{R}_{01} = 5.1891e-04$, $\mathcal{R}_{02} = 1.1290e-04$, and $\mathcal{R}_{03} = 3.6456$ have been calculated with the aid of real data in the U.K. from November 28, 2021 to December 23, 2021. In Fig. 1, the red solid circles indicate the real Omicron cases, while the best-fitted curve of the model is represented by the blue solid line.

8. Numerical scheme for the provided COVID-19 model in the Caputo derivative sense

To investigate the dynamics of the proposed fractional order model (5), we implement the Caputo fractional operator. To provide the numerical simulation of the suggested nonlinear fractional order system, the Adams type estimator-corrector method [42–45] is used. The following Cauchy-type ODE is taken into account with respect to the Caputo operator of order ϑ:

$$ {}_0^C D_t^{\vartheta} \Phi(t) = \phi(t, \Phi(t)), \quad \Phi^{(b)}(0) = \Phi_0^b, \quad 0 < \vartheta \leq 1, \quad 0 < t \leq \tau, \tag{14}$$

where $b = 0, 1, \ldots, n-1$, and $n = \lceil \vartheta \rceil$. Eq. (14) can be turned to the Volterra equation:

$$\Phi(t) = \sum_{b=0}^{n-1} \Phi_0^{(b)} \frac{t^b}{b!} + \frac{1}{\Gamma(\vartheta)} \int_0^t (t-s)^{\vartheta-1} \Phi(s, \Phi(s)) ds. \tag{15}$$

By considering this proposed predictor-corrector scheme associated with the Adam–Bashforth–Moulton algorithm [43] to have the numerical solutions of the proposed model, we can take $h=\tau/N$, $t_z=zh$, and $z=0,1,\ldots,N\in Z^+$, by letting $\Phi_z\approx\Phi(t_z)$, it can be discretized as follows, i.e., the corresponding corrector formula [46]:

$$\begin{aligned}
S_{q+1}&=\sum_{z=0}^{q-1}S_0^{(z)}\frac{t_{q+1}^z}{z!}+\frac{h^\vartheta}{\Gamma(\vartheta+2)}\sum_{z=0}^{q}\left(p_{z,q+1}\right)(\Lambda^\vartheta-\left(\mu^\vartheta+\gamma_1^\vartheta+\gamma_2^\vartheta\right)S_z-\beta_1^\vartheta\frac{S_zE_z}{N}-\beta_2^\vartheta\frac{S_zI_z}{N}-\beta_3^\vartheta\frac{S_zO_z}{N}),\\
&+\frac{h^\vartheta}{\Gamma(\vartheta+2)}\sum_{z=0}^{q}\left(p_{q+1,q+1}\right)(\Lambda^\vartheta-\left(\mu^\vartheta+\gamma_1^\vartheta+\gamma_2^\vartheta\right)S_{q+1}^{PF}-\beta_1^\vartheta\frac{S_{q+1}^{PF}E_{q+1}^{PF}}{N}-\beta_2^\vartheta\frac{S_{q+1}^{PF}I_{q+1}^{PF}}{N}-\beta_3^\vartheta\frac{S_{q+1}^{PF}O_{q+1}^{PF}}{N}),\\
E_{q+1}&=\sum_{z=0}^{q-1}E_0^{(z)}\frac{t_{q+1}^z}{z!}+\frac{h^\vartheta}{\Gamma(\vartheta+2)}\sum_{z=0}^{q}\left(p_{z,q+1}\right)(\beta_1^\vartheta\left(1-\varepsilon_1^\vartheta-\varepsilon_2^\vartheta\right)\frac{S_zE_z}{N}-\left(\mu^\vartheta+\alpha_1^\vartheta+\theta_1^\vartheta+\sigma^\vartheta\right)E_z)\\
&+\frac{h^\vartheta}{\Gamma(\vartheta+2)}\sum_{z=0}^{q}\left(p_{q+1,q+1}\right)(\beta_1^\vartheta\left(1-\varepsilon_1^\vartheta-\varepsilon_2^\vartheta\right)\frac{S_{q+1}^{PF}E_{q+1}^{PF}}{N}-\left(\mu^\vartheta+\alpha_1^\vartheta+\theta_1^\vartheta+\sigma^\vartheta\right)E_{q+1}^{PF}),\\
I_{q+1}&=\sum_{z=0}^{q-1}I_0^{(z)}\frac{t_{q+1}^z}{z!}+\frac{h^\vartheta}{\Gamma(\vartheta+2)}\sum_{z=0}^{q}\left(p_{z,q+1}\right)(\beta_1^\vartheta\varepsilon_1^\vartheta\frac{S_zE_z}{N}+\beta_2^\vartheta\frac{S_zI_z}{N}+\alpha_1^\vartheta E_z-\left(\mu^\vartheta+\alpha_2^\vartheta+\theta_2{}^\vartheta+\delta_1^\vartheta+\delta_2^\vartheta\right)I_z)\\
&+\frac{h^\vartheta}{\Gamma(\vartheta+2)}\sum_{z=0}^{q}\left(p_{q+1,q+1}\right)(\beta_1^\vartheta\varepsilon_1^\vartheta\frac{S_{q+1}^{PF}E_{q+1}^{PF}}{N}+\beta_2^\vartheta\frac{S_{q+1}^{PF}I_{q+1}^{PF}}{N}+\alpha_1^\vartheta E_{q+1}^{PF}-\left(\mu^\vartheta+\alpha_2^\vartheta+\theta_2{}^\vartheta+\delta_1^\vartheta+\delta_2^\vartheta\right)I_{q+1}^{PF}),\\
O_{q+1}&=\sum_{z=0}^{q-1}O_0^{(z)}\frac{t_{q+1}^z}{z!}+\frac{h^\vartheta}{\Gamma(\vartheta+2)}\sum_{z=0}^{q}\left(p_{z,q+1}\right)(\beta_1^\vartheta\varepsilon_2^\vartheta\frac{S_zE_z}{N}+\beta_3^\vartheta\frac{S_zO_z}{N}+\sigma^\vartheta E_z-\left(\mu^\vartheta+\alpha_3^\vartheta+\theta_3{}^\vartheta+\delta_3^\vartheta+\delta_4^\vartheta\right)O_z)\\
&+\frac{h^\vartheta}{\Gamma(\vartheta+2)}\sum_{z=0}^{q}\left(p_{q+1,q+1}\right)(\beta_1^\vartheta\varepsilon_2^\vartheta\frac{S_{q+1}^{PF}E_{q+1}^{PF}}{N}+\beta_3^\vartheta\frac{S_{q+1}^{PF}O_{q+1}^{PF}}{N}+\sigma^\vartheta E_{q+1}^{PF}-\left(\mu^\vartheta+\alpha_3^\vartheta+\theta_3{}^\vartheta+\delta_3^\vartheta+\delta_4^\vartheta\right)O_{q+1}^{PF}),\\
R_{q+1}&=\sum_{z=0}^{q-1}R_0^{(z)}\frac{t_{q+1}^z}{z!}+\frac{h^\vartheta}{\Gamma(\vartheta+2)}\sum_{z=0}^{q}\left(p_{z,q+1}\right)(\alpha_2^\vartheta I_z+\alpha_3^\vartheta O_z-\gamma_3^\vartheta R_z-\mu^\vartheta R_z)\\
&+\frac{h^\vartheta}{\Gamma(\vartheta+2)}\sum_{z=0}^{q}\left(p_{q+1,q+1}\right)(\alpha_2^\vartheta I_{q+1}^{PF}+\alpha_3^\vartheta O_{q+1}^{PF}-\gamma_3^\vartheta R_{q+1}^{PF}-\mu^\vartheta R_{q+1}^{PF}),\\
K_{q+1}&=\sum_{z=0}^{q-1}K_0^{(z)}\frac{t_{q+1}^z}{z!}+\frac{h^\vartheta}{\Gamma(\vartheta+2)}\sum_{z=0}^{q}\left(p_{z,q+1}\right)((1-\tau^\vartheta)\gamma_1^\vartheta S_z+\theta_1^\vartheta E_z+\theta_2^\vartheta I_z+\theta_3^\vartheta O_z-\mu^\vartheta K_z)\\
&+\frac{h^\vartheta}{\Gamma(\vartheta+2)}\sum_{z=0}^{q}\left(p_{q+1,q+1}\right)((1-\tau^\vartheta)\gamma_1^\vartheta S_{q+1}^{PF}+\theta_1^\vartheta E_{q+1}^{PF}+\theta_2^\vartheta I_{q+1}^{PF}+\theta_3^\vartheta O_{q+1}^{PF}-\mu^\vartheta K_{q+1}^{PF}),\\
H_{q+1}&=\sum_{z=0}^{q-1}H_0^{(z)}\frac{t_{q+1}^z}{z!}+\frac{h^\vartheta}{\Gamma(\vartheta+2)}\sum_{z=0}^{q}\left(p_{z,q+1}\right)((\gamma_2^\vartheta+\tau^\vartheta\gamma_1^\vartheta)S_z+\delta_2^\vartheta I_z+\delta_4^\vartheta O_z+\gamma_3^\vartheta R_z-(\mu_2^\vartheta+\mu^\vartheta)H_z)\\
&+\frac{h^\vartheta}{\Gamma(\vartheta+2)}\sum_{z=0}^{q}\left(p_{q+1,q+1}\right)((\gamma_2^\vartheta+\tau^\vartheta\gamma_1^\vartheta)S_{q+1}^{PF}+\delta_2^\vartheta I_{q+1}^{PF}+\delta_4^\vartheta O_{q+1}^{PF}+\gamma_3^\vartheta R_{q+1}^{PF}-(\mu_2^\vartheta+\mu^\vartheta)H_{q+1}^{PF}),
\end{aligned}$$

where

$$\begin{aligned}
S_{q+1}^{PF}&=\sum_{z=0}^{q-1}S_0^{(z)}\frac{t_{q+1}^z}{z!}+\frac{h^\vartheta}{\Gamma(\vartheta+1)}\sum_{z=0}^{q}\left(j_{z,q+1}\right)(\Lambda^\vartheta-\left(\mu^\vartheta+\gamma_1^\vartheta+\gamma_2^\vartheta\right)S_z-\beta_1^\vartheta\frac{S_zE_z}{N}-\beta_2^\vartheta\frac{S_zI_z}{N}-\beta_3^\vartheta\frac{S_zO_z}{N}),\\
E_{q+1}^{PF}&=\sum_{z=0}^{q-1}E_0^{(z)}\frac{t_{q+1}^z}{z!}+\frac{h^\vartheta}{\Gamma(\vartheta+1)}\sum_{z=0}^{q}\left(j_{z,q+1}\right)(\beta_1^\vartheta\left(1-\varepsilon_1^\vartheta-\varepsilon_2^\vartheta\right)\frac{S_zE_z}{N}-\left(\mu^\vartheta+\alpha_1^\vartheta+\theta_1^\vartheta+\sigma^\vartheta\right)E_z),\\
I_{q+1}^{PF}&=\sum_{z=0}^{q-1}I_0^{(z)}\frac{t_{q+1}^z}{z!}+\frac{h^\vartheta}{\Gamma(\vartheta+1)}\sum_{z=0}^{q}\left(j_{z,q+1}\right)(\beta_1^\vartheta\varepsilon_1^\vartheta\frac{S_zE_z}{N}+\beta_2^\vartheta\frac{S_zI_z}{N}+\alpha_1^\vartheta E_z-\left(\mu^\vartheta+\alpha_2^\vartheta+\theta_2{}^\vartheta+\delta_1^\vartheta+\delta_2^\vartheta\right)I_z),\\
O_{q+1}^{PF}&=\sum_{z=0}^{q-1}O_0^{(z)}\frac{t_{q+1}^z}{z!}+\frac{h^\vartheta}{\Gamma(\vartheta+1)}\sum_{z=0}^{q}\left(j_{z,q+1}\right)(\beta_1^\vartheta\varepsilon_2^\vartheta\frac{S_zE_z}{N}+\beta_3^\vartheta\frac{S_zO_z}{N}+\sigma^\vartheta E_z-\left(\mu^\vartheta+\alpha_3^\vartheta+\theta_3{}^\vartheta+\delta_3^\vartheta+\delta_4^\vartheta\right)O_z),\\
R_{q+1}^{PF}&=\sum_{z=0}^{q-1}R_0^{(z)}\frac{t_{q+1}^z}{z!}+\frac{h^\vartheta}{\Gamma(\vartheta+1)}\sum_{z=0}^{q}\left(j_{z,q+1}\right)(\alpha_2^\vartheta I_z+\alpha_3^\vartheta O_z-\gamma_3^\vartheta R_z-\mu^\vartheta R_z),\\
K_{q+1}^{PF}&=\sum_{z=0}^{q-1}K_0^{(z)}\frac{t_{q+1}^z}{z!}+\frac{h^\vartheta}{\Gamma(\vartheta+1)}\sum_{z=0}^{q}\left(j_{z,q+1}\right)((1-\tau^\vartheta)\gamma_1^\vartheta S_z+\theta_1^\vartheta E_z+\theta_2^\vartheta I_z+\theta_3^\vartheta O_z-\mu^\vartheta K_z),
\end{aligned}$$

$$H_{q+1}^{PF} = \sum_{z=0}^{q-1} H_0^{(z)} \frac{t_{q+1}^z}{z!} + \frac{h^\vartheta}{\Gamma(\vartheta+1)} \sum_{z=0}^{q} \left(j_{z,q+1}\right)((\gamma_2^\vartheta + \tau^\vartheta \gamma_1^\vartheta) S_z + \delta_2^\vartheta I_z + \delta_4^\vartheta O_z + \gamma_3^\vartheta R_z - (\mu_2^\vartheta + \mu^\vartheta) H_z),$$

and

$$p_{z,q+1} = \begin{cases} q^{\vartheta+1} - (q-\vartheta)(q+1)^\vartheta, & \text{if } z = 0, \\ (q-z+2)^{\vartheta+1} + (q-z)^{\vartheta+1} - 2(q-z+1)^{\vartheta+1}, & \text{if } 1 \le z \le q, \\ 1, & \text{if } z = q+1, \end{cases} \tag{16}$$

where

$$j_{z,q+1} = (q+1-z)^\vartheta - (q-z)^\vartheta.$$

9. Memory trace and hereditary traits

To examine the behaviour of the model (5), the Caputo operator have been used that defined in (1). For ϑ, $0 < \vartheta \le 1$ derivative, let the fractional derivative of variable $\Phi(t)$ be [37,39]

$${}_0^C D_t^\vartheta \Phi(t) = H(\Phi(t), t), \tag{17}$$

where H is a continuous function. Utilizing the L1 scheme, Naik et al. [38], Jin et al. [39], Du and Wang [40], Magin [41], the numerical approximation of FOD of $\Phi(t)$ is

$${}_0^C D_t^\vartheta \Phi(t) \approx \frac{(dt)^{-\vartheta}}{\Gamma(2-\vartheta)} \left[\sum_{\varrho=0}^{T-1} \left[\Phi\left(t_{\varrho+1}\right) - \Phi\left(t_\varrho\right)\right]\left[(T-\varrho)^{1-\vartheta} - (T-1-\varrho)^{1-\vartheta}\right] \right]. \tag{18}$$

The purpose of applying the L1 scheme to our study is its memory term and convergence rate. Memory term is also clearly presented in other numerical methods, but this memory integration term is more explicitly described in the L1 scheme. Taking into considering (17) and (18) together, the numerical solution of (17) is as follows:

$$\Phi(t_T) \approx {}_0^C D_t^\vartheta \Gamma(2-\vartheta) H(\Phi(t), t) + \Phi(t_{T-1}) - \left[\sum_{\varrho=0}^{T-2} \left[\Phi\left(t_{\varrho+1}\right) - \Phi\left(t_\varrho\right)\right]\left[(T-\varrho)^{1-\vartheta} - (T-1-\varrho)^{1-\vartheta}\right] \right]. \tag{19}$$

Therefore, the solution of the FOD can be represented as the difference between the Markov term and the memory trace. The Markov term weighted by the Gamma function as follows:

$$\text{Markov term} = {}_0^C D_t^\vartheta \Gamma(2-\vartheta) H(\Phi(t), t) + \Phi(t_{T-1}). \tag{20}$$

The memory trace (Φ-memory trace since it is related to variable $\Phi(t)$) is

$$\text{Memory trace} = \sum_{\varrho=0}^{T-2} \left[\Phi\left(t_{\varrho+1}\right) - \Phi\left(t_\varrho\right)\right]\left[(T-\varrho)^{1-\vartheta} - (T-1-\varrho)^{1-\vartheta}\right]. \tag{21}$$

The memory trace shows us all of the past activities and a long-term history of our model. For $\vartheta = 1$, the memory trace is 0 for any time t. The dynamics of the memory trace is highly time-dependent. When the fractional order ϑ decreases from unity, the memory trace increases nonlinearly from 0. This tells us how different the fractional order model is from the integer order model.

10. Numerical simulations and discussion

In this section, we provide the numerical solution to the model (5), using the Adams–Bashforth–Moulton Predictor-Corrector method for the values in Table 1. By means of numerical solutions, which parameters play an active role in the spread of the disease and which ϑ values reveal the best memory effect have been examined. Therefore, the variation of each sub-population over time has been simulated for different values of ϑ by using the values given in Table 1. Additionally, taking into account parameters that significantly change the behavior of system dynamics, graphics have been obtained for various values of these parameters. The dynamical behaviour of each state of the proposed COVID-19 pandemic and heart attack model has shown in Figs. 2–15 for varying values of ϑ and different parameter values. Fig. 2 demonstrates the susceptible individuals for different ϑ values to observe the most significant fractional-order. In this figure, we see that susceptible individuals exhibit a decreasing attitude until approximately the 40th day and then display a almost stable behavior, for increasing values of ϑ. This behavior of susceptible individuals is inevitable as a result of the emergence and rapid transmission of the Omicron variant (about 70 times faster than other variants of COVID-19).

In Fig. 3, the exposed individuals change according to the change of time is showed. One can see from this figure that the exposed individuals show an increase until the day when the behavior of susceptible individuals changes from decreasing to stability, and after that day, the exposed individuals show decreasing behavior. In addition, The lower the value ϑ from the unit, the memory effect of the system increases. Thus, exposed individuals need more time to be stable for non-integer cases.

In Fig. 4, it has been observed that the infectious increases until the approximately 25th day, then begins to decrease and it will reach stability after a certain time. According to this figure, the number of infected individuals in the community on the 200th day is estimated to be 13755. For $\vartheta = 0.91$ at the integer-order case, the number of infected individuals is defined as 4211. Thus, the fractional-order predicts about 9544 infectious cases, which is more than the prediction resulting from using the integer-order. Beside that, when $\vartheta = 0.91$, It has been calculated that the infected individuals disappeared from the society on the 720th day for the integer-order, whereas for $\vartheta = 0.91$, there are still 1553 infected individuals in the society. That is a pretty and effective forecast for the course of COVID-19.

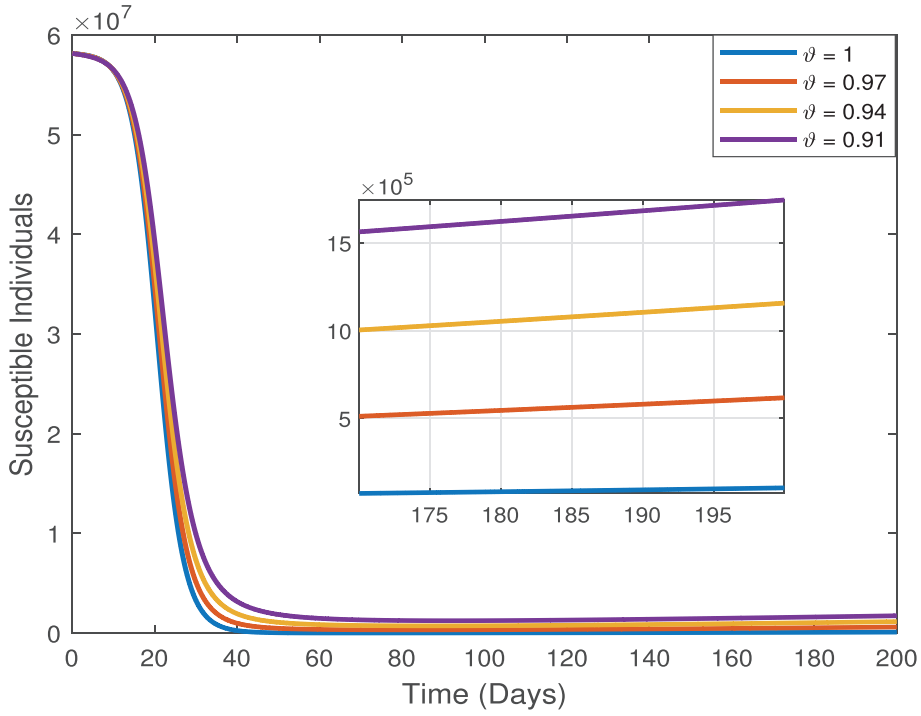

Fig. 2. Change of Susceptible individuals over time for the varying fractional-order derivative.

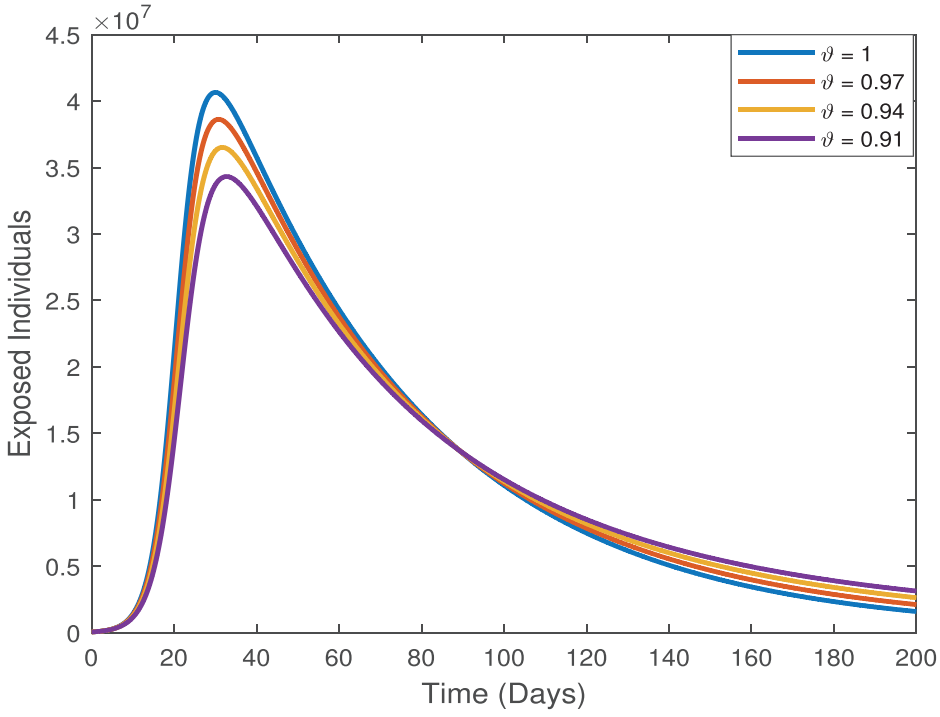

Fig. 3. Change of Exposed individuals over time for the varying fractional-order derivative.

In Fig. 5, an almost similar behavior is observed as in Fig. 4. However, it takes longer time for infected individuals with the omicron variant to reach the peak value and equilibrium point compared to class *I*. When Fig. 5 is examined in detail, it appears from that the estimation of disease calculated for the fractional order at any time is stronger than the estimation of the integer-order derivative. For example, for $\vartheta = 1, 0.97, 0.94, 0.91$ at day 633, 0, 62, 228 and 511 infected individuals are estimated, respectively. There is a difference of 511 people between the number estimated for $\vartheta = 0.91$ and the number estimated for $\vartheta = 1$. This is a critical estimate for such an important disease.

In Fig. 6, the variation of recovered individuals over time has been displayed. It is seen that they exhibit a decreasing behavior first, then increasing and then decreasing again. The decrease in the recovered population is due to individuals who have had a heart attack and individuals who have died naturally. In Fig. 7, It is clear that the number of individuals in quarantine has increased over time. In Fig. 8, there is a sudden in-

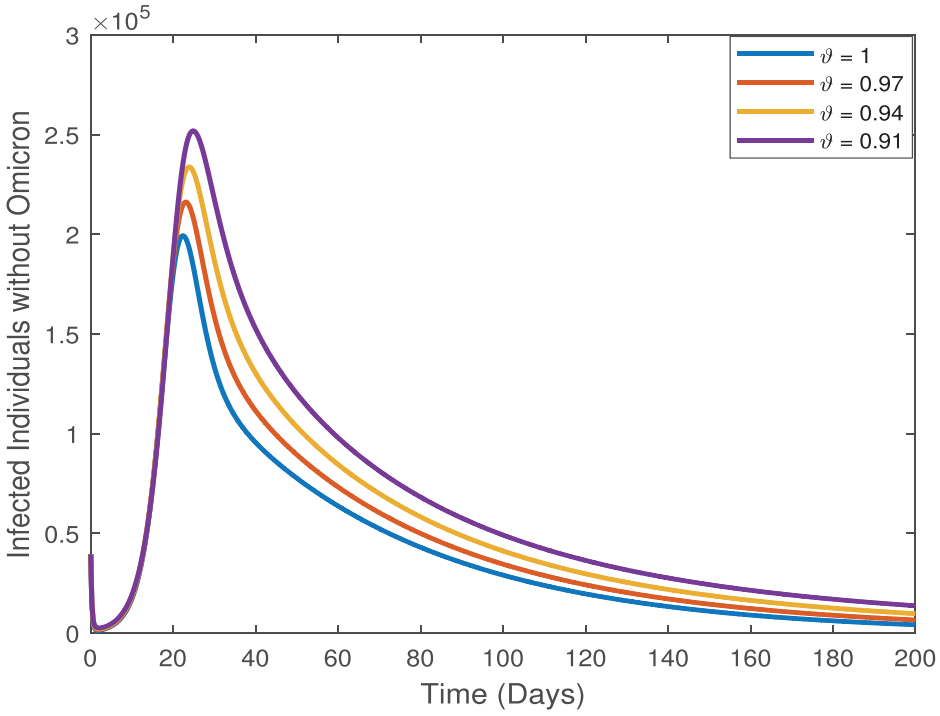

Fig. 4. Change of Infected individuals without Omicron variant over time for the varying fractional-order derivative.

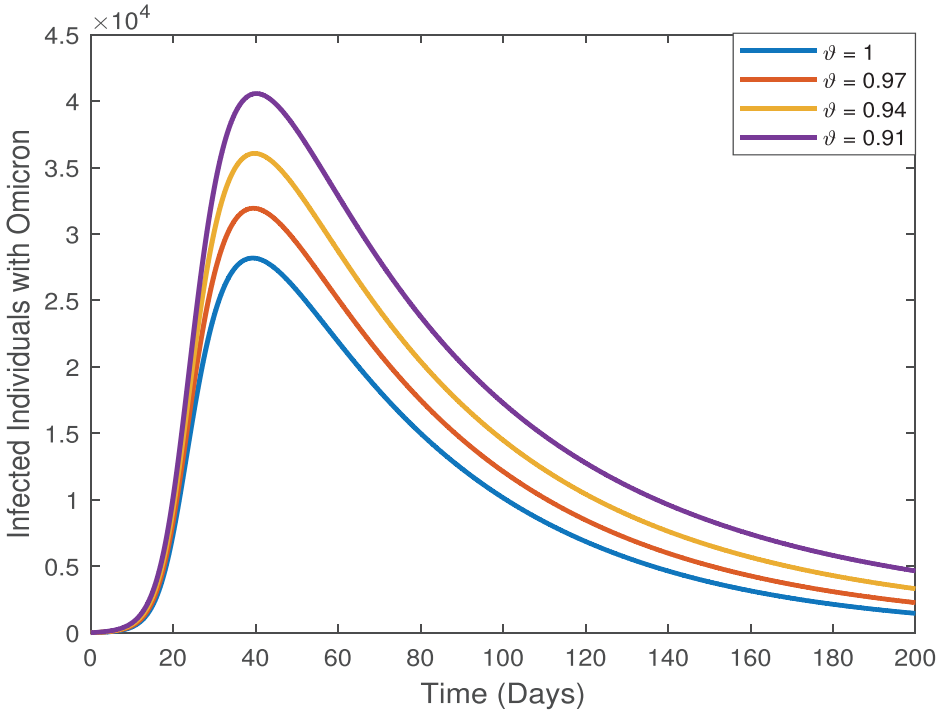

Fig. 5. Change of Infected individuals with Omicron variant over time for the varying fractional-order derivative.

crease at first, then a decrease, in the number of people who have had a heart attack, then an increase again, and a trend towards stability after a final decrease is noteworthy. It is clear that the observed changes in Figs. 2–8 are compatible with the expected phenomena respect to a real COVID-19 and Omicron variant.

In Fig. 9, we have changed β_1 and keep the other parameters fixed as in Table 1. It is seen that in Fig. 9, as β_1 increases, the number of exposed individuals increases and as β_1 decreases the number of exposed individuals decreases. In Fig. 10, with the increase of β_2 (the rate of disease transmission through contact with I class, the number of infected individuals also increases. Similarly, it is seen that in Figs. 11 and 12, as β_1 and β_3 increases, a significant increase is observed in O class.

From the biological point of view, if the rate of disease transmission through contact with E, I, O classes (β_1, β_2, β_3) can be

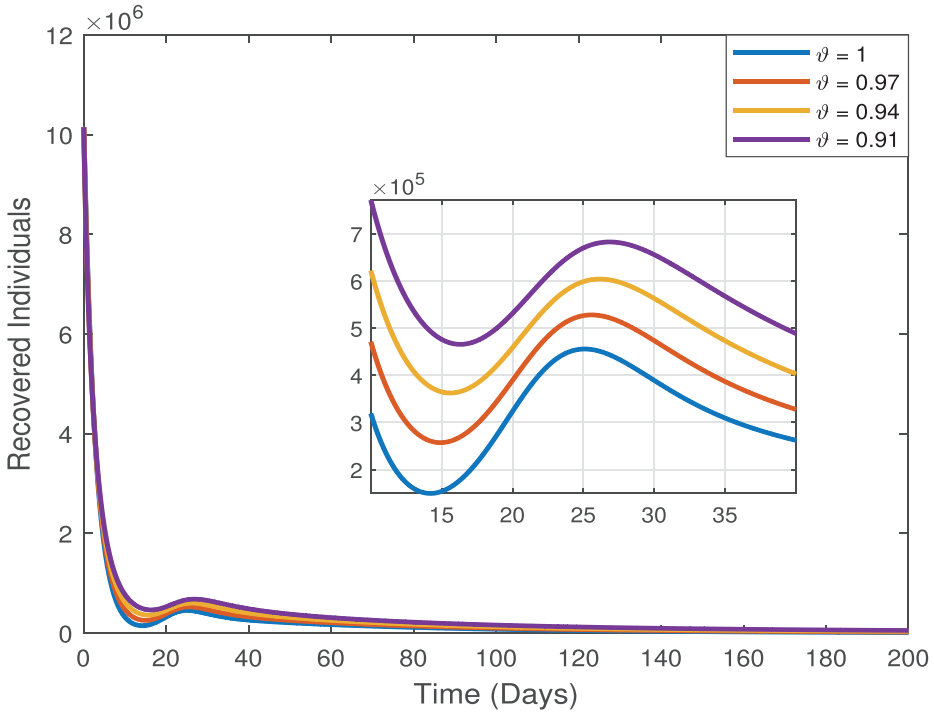

Fig. 6. Change of Recovered individuals over time for the varying fractional-order derivative.

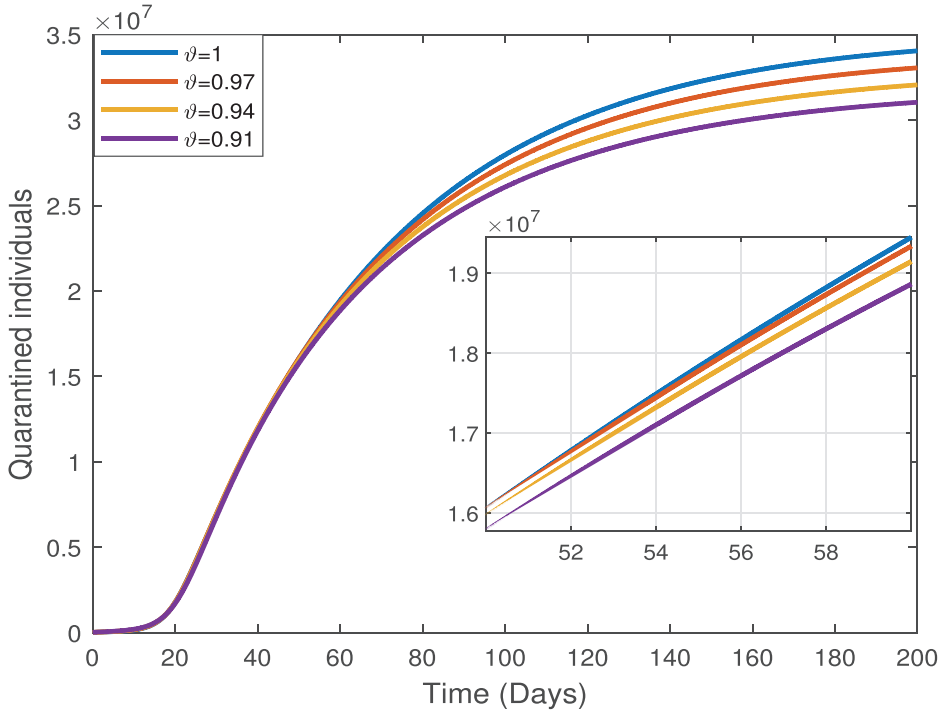

Fig. 7. Change of Quarantined individuals over time for the varying fractional-order derivative.

decreased by the lock-down then there will be a significant reduction in the number of exposed individuals (E class), infected individuals without omicron (I class) variant and infected individuals with omicron variant (O class). In Figs. 13 and 14, the changes in O class and K class according to δ_4 and β_1 have been examined. As expected, the increase in δ_4 causes a decrease in the O class. Along with the increase in β_1, a remarkable increase in the K class draws attention. In Fig. 15, the time-dependent variation of the heart attack class has been investigated for different values of γ_1 and γ_2. It is expected that the number of H class biologically will increase with the increase of γ_1 and γ_2. Thus, the results obtained in the figures are consistent with the results expected from the constructed model.

In Figs. 16–19, we have showed how the memory effect in each sub-population changes as ϑ takes different values. In these figures, it is seen that when $\vartheta = 1$ takes the value of zero, that

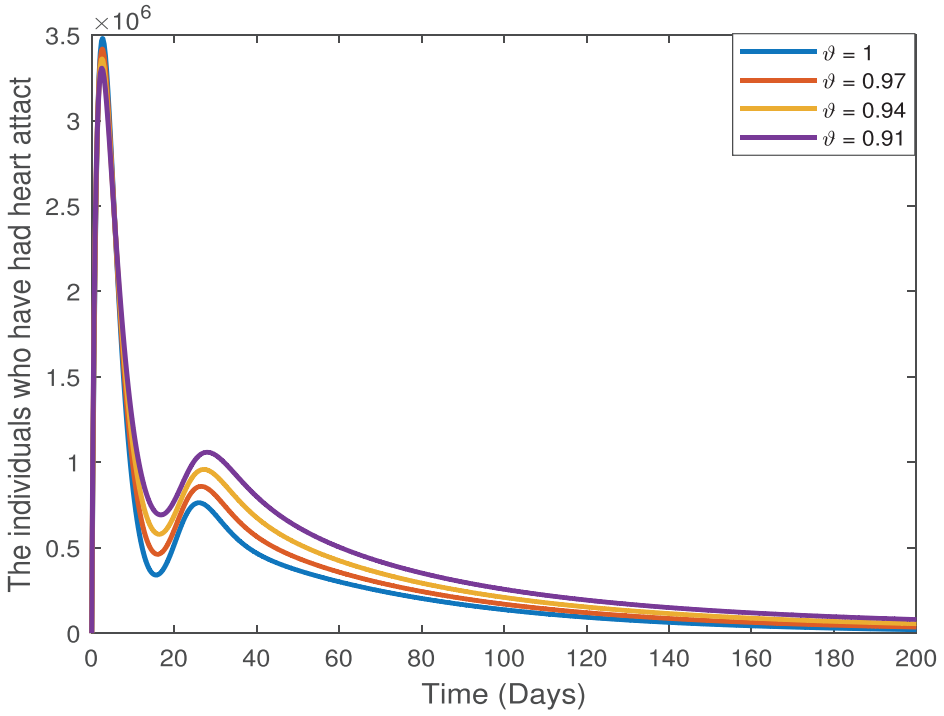

Fig. 8. Change of individuals who have had a heart attack over time for the varying fractional-order derivative.

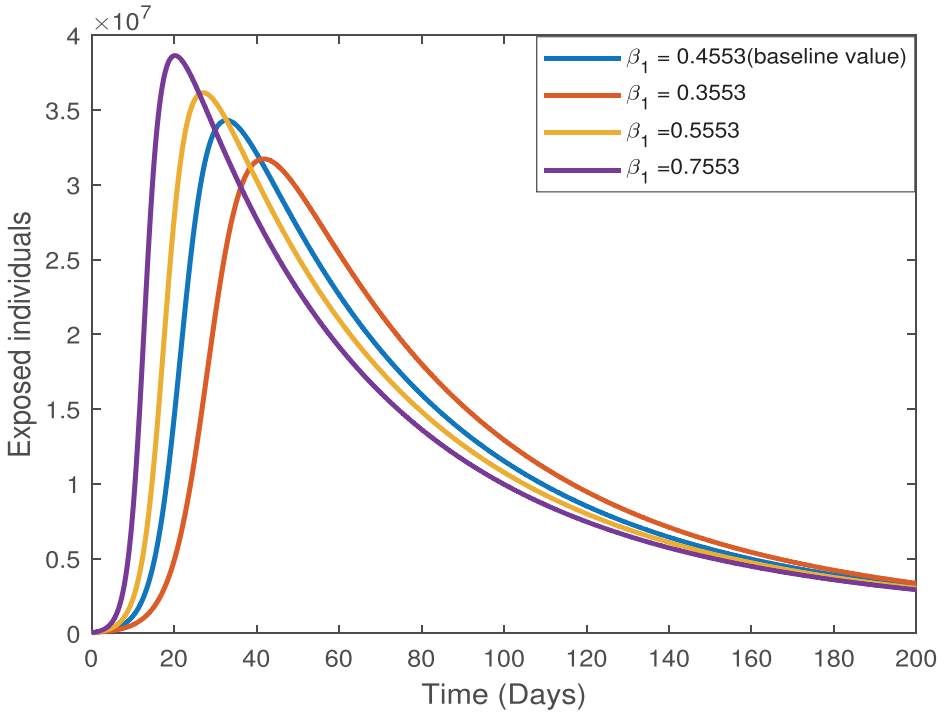

Fig. 9. Change of the exposed individuals over time for the different β_1 values and $\vartheta = 0.91$.

is, in the case of integer order, the memory effect is zero. However, when ϑ takes on fractional order values, the memory effect present in the fractional derivative begins to appear. It is observed that the corresponding memory effect exhibits an increasing behavior as ϑ decreases from 1 to 0.91. Since there is a memory effect in the structure of infectious diseases, it is necessary to include the memory effect in the system in order to create the most realistic mathematical model. The fractional derivatives used in the mathematical model we constructed clearly show the memory effect present in each population of the system in Figs. 16–19. When attention is paid to the before and after the peak values of the populations, it is seen that there is a significant relationship between them and the Figs. 2–15. In addition, when Figs. 2–15 and 16–19 are considered together, it is note that memory trace is negative when populations decrease, and memory trace is positive when populations increase. Observing such behaviors clearly shows how important the inclusion of memory traces in the system is in modeling infectious diseases.

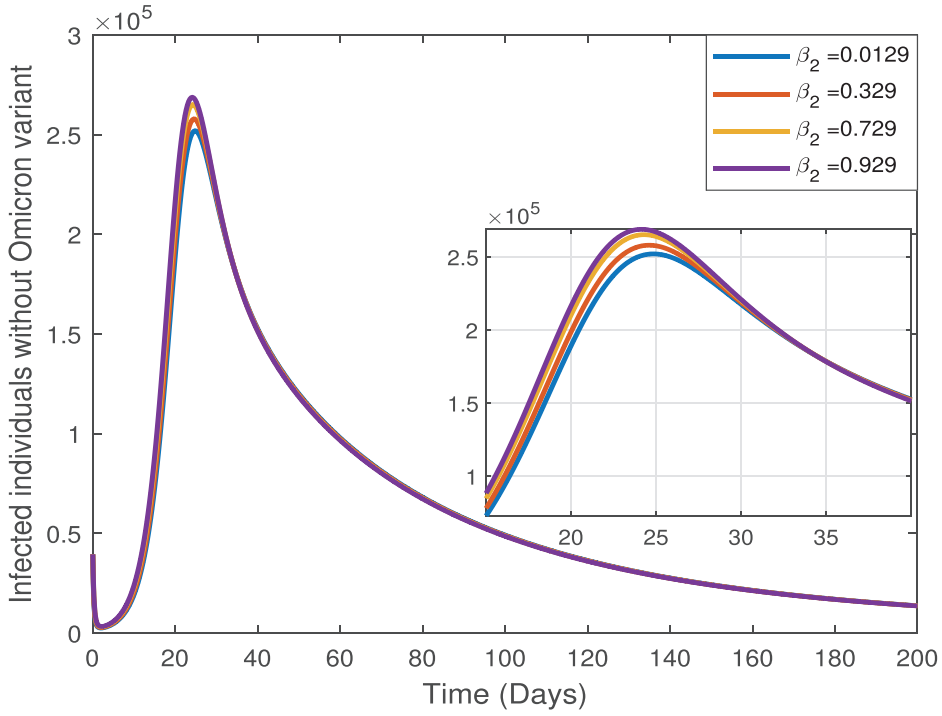

Fig. 10. Change of the infected individuals without Omicron variant over time for the different β_2 values and $\vartheta = 0.91$.

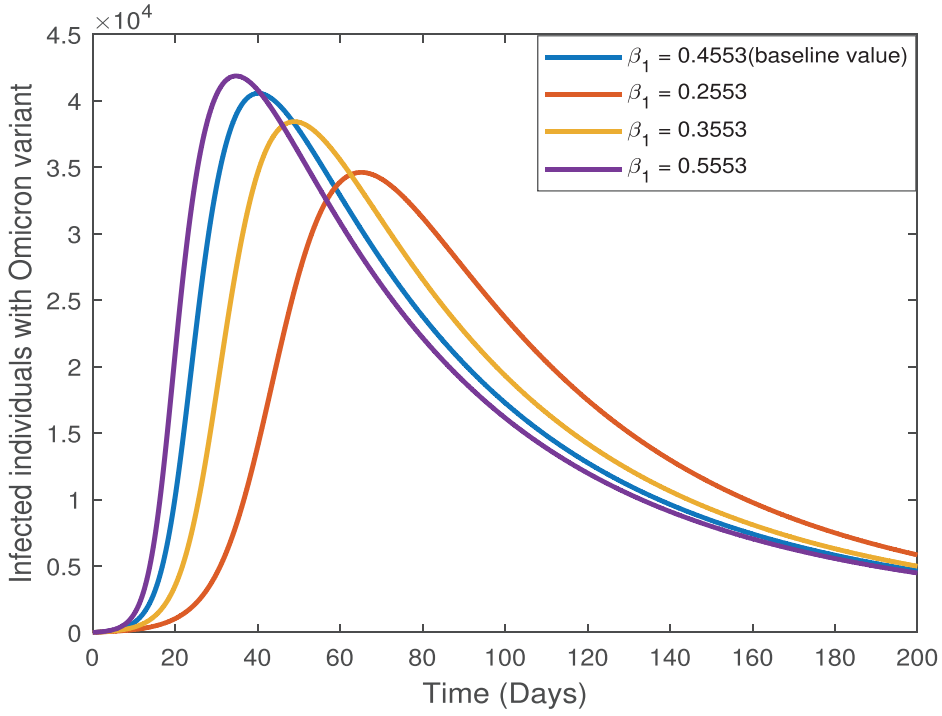

Fig. 11. Change of the infected individuals with Omicron variant over time for the different β_1 values and $\vartheta = 0.91$.

11. Measurement of memory trace for the proposed fractional-order model

The fractional derivatives have been numerically integrated by using the L1 scheme and the solutions of the FODEs for $S(t), E(t), I(t), O(t), R(t), K(t), H(t)$ have been depicted as the similar way as in (9), as given in detail in Section 9. Therefore, the numerical approximation of the FOD of $S(t)$ is

$$
\begin{aligned}
&{}_0^C D_t^{\vartheta} S(t) \\
&\approx \frac{(dt)^{-\vartheta}}{\Gamma(2-\vartheta)}\left[\sum_{\varrho=0}^{T-1}\left[S\left(t_{\varrho+1}\right)-S\left(t_{\varrho}\right)\right]\left[(T-\varrho)^{1-\vartheta}-(T-1-\varrho)^{1-\vartheta}\right]\right].
\end{aligned} \tag{22}
$$

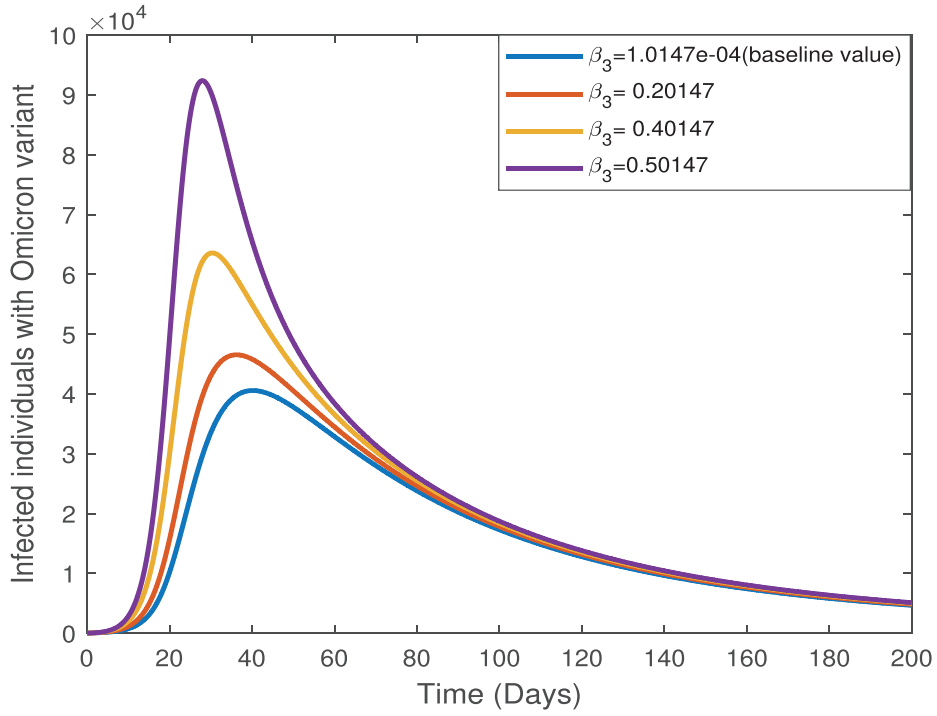

Fig. 12. Change of the infected individuals with Omicron variant over time for the different β_3 values and $\vartheta = 0.91$.

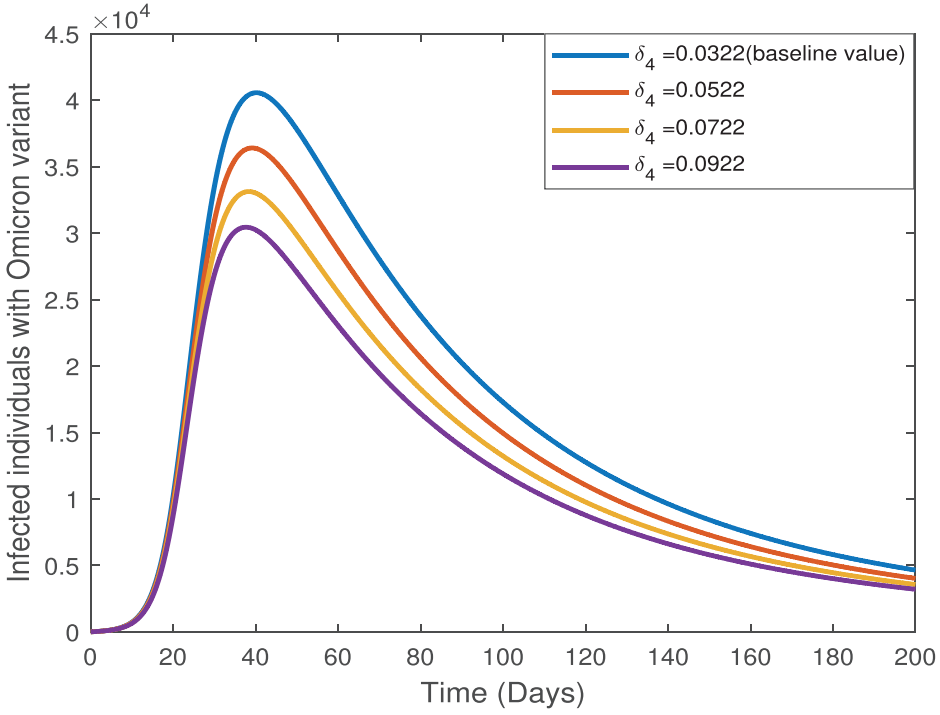

Fig. 13. Change of the infected individuals with Omicron variant over time for the different δ_4 values and $\vartheta = 0.91$.

By combining (22) and the first equation of system, the numerical solution of $S(t)$ is given by

$$S(t_T) \approx \text{Markov term of } S(t) \text{- Memory trace of } S(t), \tag{23}$$

where

$$\text{Markov term} = {}_0^C D_t^{\vartheta}\, \Gamma(2-\vartheta) H(S(t), t) + S(t_{T-1}), \tag{24}$$

and

$$\text{Memory trace} = \sum_{\varrho=0}^{T-2} \left[S\left(t_{\varrho+1}\right) - S\left(t_{\varrho}\right) \right] \left[(T-\varrho)^{1-\vartheta} - (T-1-\varrho)^{1-\vartheta} \right]. \tag{25}$$

Applying the same steps, the numerical approximations of the FOD (fractional-order derivative) of $E(t)$, $I(t)$, $O(t)$, $R(t)$, $K(t)$, $H(t)$ have been achieved. It is seen from the previous results, numerical anal-

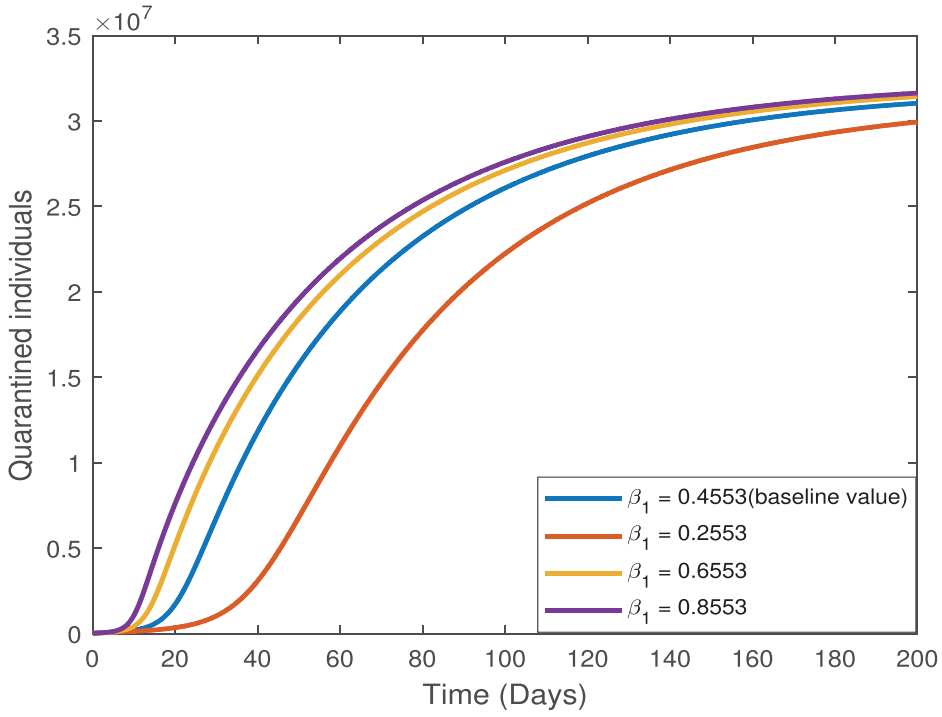

Fig. 14. Change of the quarantined individuals over time for the different β_1 values and $\vartheta = 0.91$.

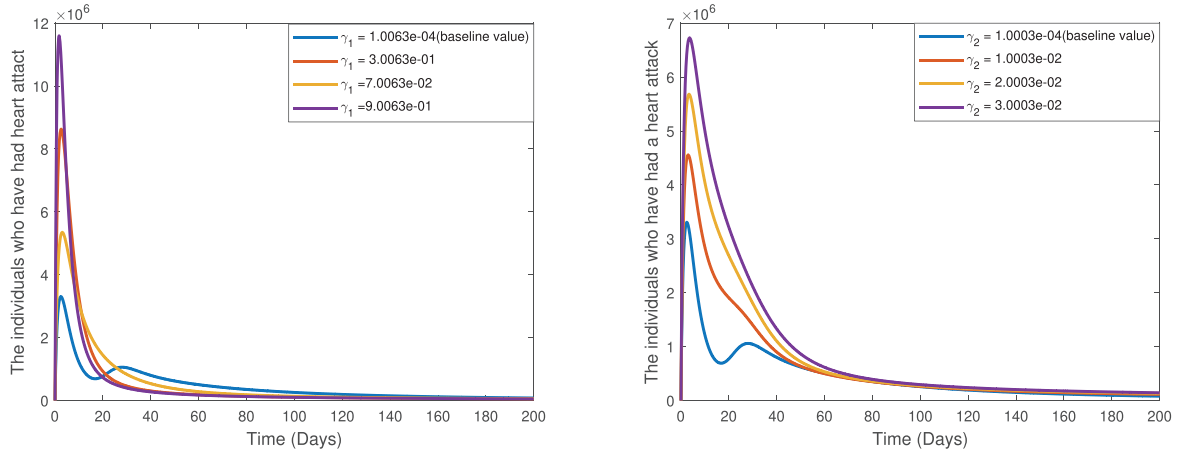

Fig. 15. Change of individuals who have had a heart attack over time for the varying γ_1 (left) and γ_2 (right) values, $\vartheta = 0.91$.

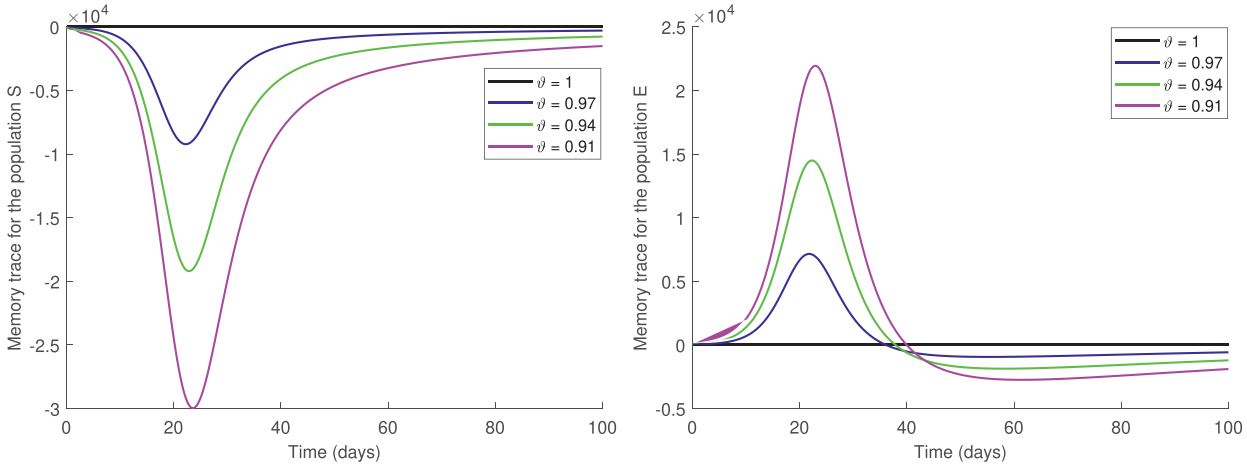

Fig. 16. The effect of memory trace on susceptible individuals (left) and exposed individuals (right) for different values of ϑ.

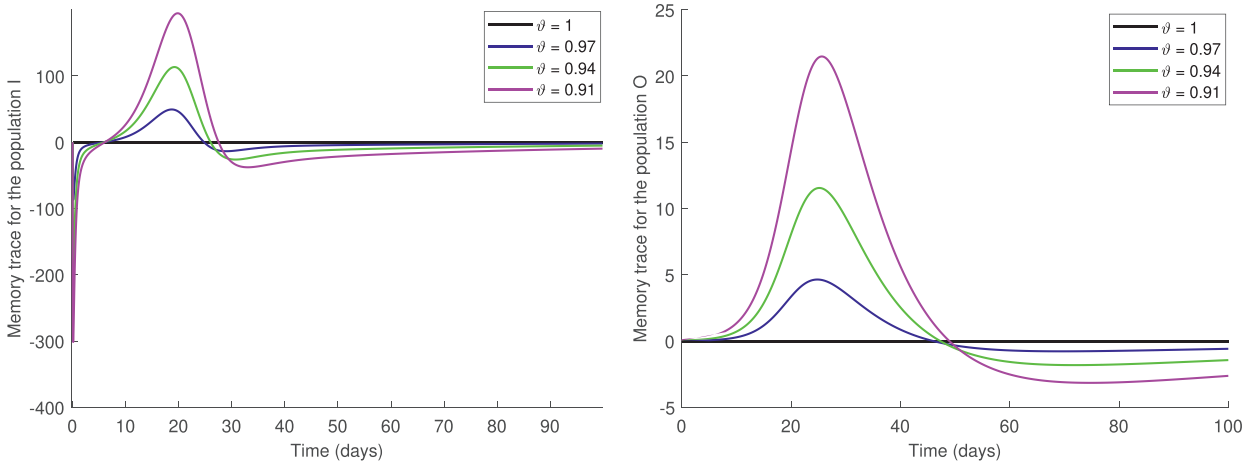

Fig. 17. The effect of memory trace on the infected individuals without omicron variant (left) and with omicron variant (right) for different values of ϑ.

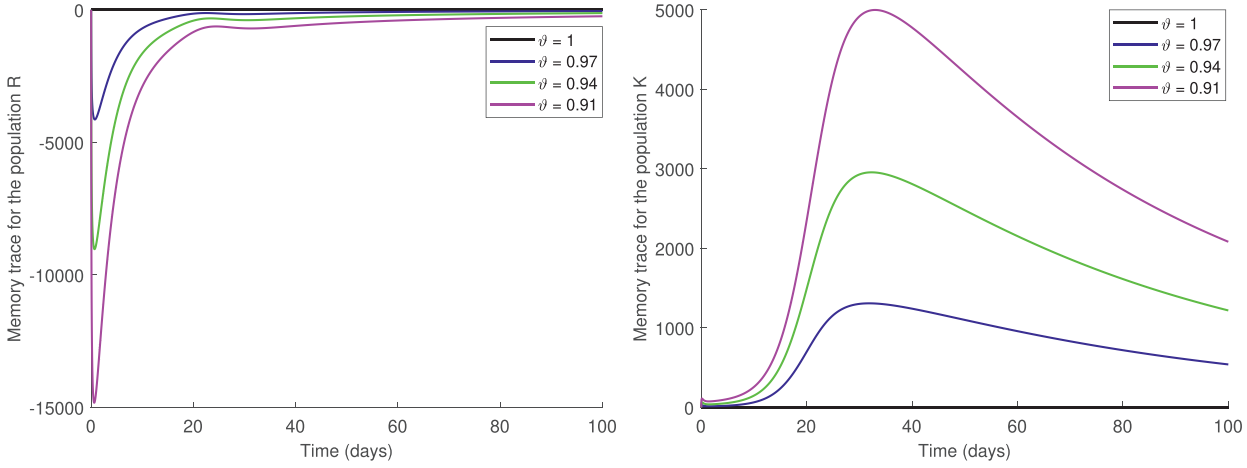

Fig. 18. The effect of memory trace on recovered individuals (left) and quarantined individuals (right) for different values of ϑ.

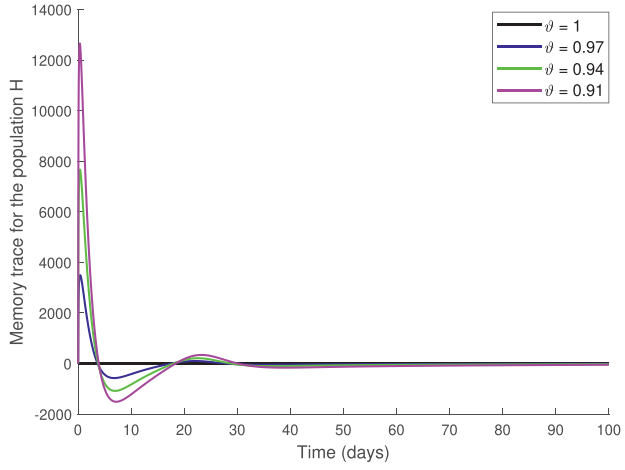

Fig. 19. The effect of memory trace on heart attack *(H)* class for different values of ϑ.

yses have been provided to visually see how each sub-population of the system (5) affected by memory tracking. The effect of memory trace on each sub-population behavior for different values of ϑ is shown in Figs. 16–19. From Figs. 16–19, when $\vartheta = 1$, it is seen that there is no memory effect in the system, that is, it is zero. From the moment ϑ started to take fractional order values, the existence of memory effect started to be seen in numerical simulations. For this reason, it is extremely important to use fractional order derivatives with memory effect in order to make the most realistic mathematical modeling and to make correct predictions. Examining Figs. 2–15 and 16–19 are together, one can see that there is a significant relationship between the peak values of the each subpopulation of the system and the memory effect. For example in Figs. 5 and 17, it is seen that where the infected individuals with omicron variant starts to decrease, the memory effect also changes direction towards negative.

In the course of infectious diseases, a memory response occurs when the immune system first encounters the virus, and this effect continues for a certain period of time [47]. It is clear from the results obtained from numerical simulations that fractional order differential equations are quite successful in detecting the memory trace of the system.

12. Conclusions

In this paper, first of all, we have given a brief information about COVID-19 and the Omicron variant. We have investigated the spread of COVID-19 and especially 'Omicron' and its effect on heart attack. Thus, we have constructed a novel Caputo fractional order model with dimensionally consistent. By using the fixed point theorem, it has been shown that the system has a solution and the equilibrium points of the system have been found. The local stability of the equilibrium points has been investigated. Then, con-

sidering real data of the Omicron variant from the United Kingdom, the sum of the squares of the difference between the numerical solution given to the Omicron-infected individuals and the real data has been minimized by LCM and the best fit curve has been obtained (see Fig. 1). In addition, with the PE method, the most compatible values of the parameters in the model have been calibrated and it has been aimed to observe the system dynamics in a better and more realistic way. By utilizing the Adams–Bashforth–Moulton method, numerical simulations of the proposed pandemic model have been visualized for different fractional orders and different parameter values. With the help of the numerical simulations, we have investigated the effect of parameters both on the increase and decrease of the heart attack class, and on the spread and regression of the pandemic. An increase in the number of people who has heart attacks is observed when Omicron cases were first seen. In the future, it is estimated that the risk of heart attack will decrease as the cases of Omicron decrease.

The Omicron variant has a different progression structure from other diseases from the moment the virus enters the body. It is seen that this different effect of the Omicron variant can be better explained with the help of fractional order equations, as can be understood from the results obtained.

The use of real data is a very useful method to test the accuracy of the constructed mathematical model. However, the main problem is usually how to find these data and/or to obtain the appropriate curve for the obtained data. Many studies have been performed on the mathematical model of COVID-19. Most of the studies are related to previous variants of COVID-19 and have not used real data. Best of our knowledge, it is noted that there is still no study in the literature on fractional modeling using real data on the Omicron variant from the United Kingdom.

In this study, a fractional order modeling has been demonstrated using real data from the U.K. related to the Omicron variant. In order to fit the parameters and reduce the absolute relative error of the curve plotted for the Omicron variant class and the real data provided by the UK, we have used the least-squares curve fitting technique. Thus, we want to foresee the population change over time using more accurately generated parameters. Moreover, we have illustrated the advantages of the fractional model considering memory tracking and hereditary traits.

According to our numerical results, if the number of contacts with infected people can be reduced through practices such as quarantine and curfew or if more people can be tested, that is, if routine tests can be performed not only on symptomatic individuals, but also on asymptomatic individuals then it will be possible to stop the spread of COVID-19 with Omicron variant. Therefore, such studies provide other scientists and specialists who study infectious diseases with insight that may benefit them to control the pandemic with its variants in the future and help develop more treatment methods. In this context, this paper may shed light on possible studies in the future. In the future, one can consider different types of fractional operators with and without singular kernels in analysis of COVID-19 containing Omicron variant.

Consent for publication

Not applicable.

Declaration of Competing Interest

The authors declare that they have no known competing financial interests or personal relationships that could have appeared to influence the work reported in this paper.

CRediT authorship contribution statement

Fatma Özköse: Conceptualization, Visualization, Methodology, Software, Writing – original draft. **Mehmet Yavuz:** Visualization, Investigation, Software, Writing – original draft. **M. Tamer Şenel:** Supervision, Software, Writing – review & editing. **Rafla Habbireeh:** Visualization, Software, Methodology, Writing – original draft.

Acknowledgements

This study was supported by Research Fund of the Erciyes University. Project Number: FDS-2021-11059. M. Yavuz was supported by TUBITAK (The Scientific and Technological Research Council of Turkey). The authors are very much thankful to the reviewers and editor for their valuable suggestions that have improved the quality of the manuscript.

References

[1] Daşbaşı B, Öztürk I, Özköse F. Mathematical modelling of bacterial competition with multiple antibiotics and it's stability analysis. Karaelmas Sci Eng J 2016;6(2):299–306.
[2] Bozkurt F, Özköse F. Stability analysis of macrophage-tumor interaction with piecewise constant arguments. In: AIP conference proceedings, vol. 1648. AIP Publishing LLC; 2015. p. 850035.
[3] Baleanu D, Abadi MH, Jajarmi A, Vahid KZ, Nieto JJ. A new comparative study on the general fractional model of COVID-19 with isolation and quarantine effects. Alex Eng J 2022;61(6):4779–91.
[4] Jajarmi A, Baleanu D, Vahid KZ, Pirouz HM, Asad JH. A new and general fractional Lagrangian approach: acapacitor microphone case study. Results Phys 2021;31:104950.
[5] Baleanu D, Zibaei S, Namjoo M, Jajarmi A. A nonstandard finite difference scheme for the modeling and nonidentical synchronization of a novel fractional chaotic system. Adv Differ Equ 2021;2021(1):308.
[6] Sene N. Second-grade fluid with newtonian heating under Caputo fractional derivative: analytical investigations via Laplace transforms. Math Model Numer Simul Appl 2022;2(1):13–25.
[7] Erturk VS, Godwe E, Baleanu D, Kumar P, Asad J, Jajarmi A. Novel fractional-order Lagrangian to describe motion of beam on nanowire. Acta Phys Polonica, A 2021;140(3):265–72.
[8] Amar NC, Bashir A. A fractional-order differential equation model of COVID-19 infection of epithelial cells. Chaos, Solitons Fractals 2021;147:110952.
[9] Özköse F, Yavuz M. Investigation of interactions between COVID-19 and diabetes with hereditary traits using real data: a case study in Turkey. Comput Biol Med 2022;141:105044.
[10] Allegretti S, Bulai IM, Marino R, Menandro MA, Parisi K. Vaccination effect conjoint to fraction of avoided contacts for a SARS-CoV-2 mathematical model. Math Model Numer Simul Appl 2021;1(2):56–66.
[11] Musa SS, Qureshi S, Zhao S, Yusuf A, Mustapha UT, He D. Mathematical modeling of COVID-19 epidemic with effect of awareness programs. Infect Dis Model 2021;6:448–60.
[12] Memon Z, Qureshi S, Memon BR. Assessing the role of quarantine and isolation as control strategies for COVID-19 outbreak: a case study. Chaos, Solitons Fractals 2021;144:110655.
[13] Peter OJ, Qureshi S, Yusuf A, Al-Shomrani M, Idowu AA. A new mathematical model of COVID-19 using real data from Pakistan. Results Phys 2021;24:104098.
[14] Naik PA, Yavuz M, Qureshi S, Zu J, Townley S. Modeling and analysis of COVID-19 epidemics with treatment in fractional derivatives using real data from Pakistan. Eur Phys J Plus 2020;135(10):1–42.
[15] Jajarmi A, Baleanu D, Zarghami Vahid K, Mobayen S. A general fractional formulation and tracking control for immunogenic tumor dynamics. Math Methods Appl Sci 2022;45(2):667–80.
[16] Öztürk I, Özköse F. Stability analysis of fractional order mathematical model of tumor-immune system interaction. Chaos, Solitons Fractals 2020;133:109614.
[17] Hammouch Z, Yavuz M, Özdemir N. Numerical solutions and synchronization of a variable-order fractional chaotic system. Math Model Numer Simul Appl 2021;1(1):11–23.
[18] Naik PA, Owolabi KM, Yavuz M, Zu J. Chaotic dynamics of a fractional order HIV-1 model involving AIDS-related cancer cells. Chaos, Solitons Fractals 2020;140:110272.
[19] Özköse F, Şenel MT, Habbireeh R. Fractional-order mathematical modelling of cancer cells-cancer stem cells-immune system interaction with chemotherapy. Math Model Numer Simul Appl 2021;1(2):67–83.
[20] Akgül A, Ahmed N, Raza A, Iqbal Z, Rafiq M, Baleanu D, et al. New applications related to COVID-19. Results Phys 2021;20:103663.
[21] Özköse F, et al. A fractional modeling of tumor-immune system interaction related to lung cancer with real data. Eur Phys J Plus 2022;137(1):1–28.

[22] Farman M, Akgül A, Nisar KS, Ahmad D, Ahmad A, Kamangar S, et al. Epidemiological analysis of fractional order COVID-19 model with Mittag–Leffler kernel. AIMS Math 2022;7(1):756–83.
[23] Joshi H, Jha BK. Chaos of calcium diffusion in Parkinson's infectious disease model and treatment mechanism via Hilfer fractional derivative. Math Model Numer Simul Appl 2021;1(2):84–94.
[24] Atangana A, Baleanu D. New fractional derivatives with nonlocal and non-singular kernel: theory and application to heat transfer model. Therm Sci 2016;20(2):763.
[25] Bonyah E, Yavuz M, Baleanu D, Kumar S. A robust study on the listeriosis disease by adopting fractal-fractional operators. Alex Eng J 2022;61(3):2016–28.
[26] Kumar P, Erturk VS. Dynamics of cholera disease by using two recent fractional numerical methods. Math Model Numer Simul Appl 2021;1(2):102–11.
[27] Uçar E, Uçar S, Evirgen F, Özdemir N. A fractional SAIDR model in the frame of Atangana–Baleanu derivative. Fractal Fract 2021;5(2):32.
[28] Mishra P, Parveen R, Bajpai R, Samim M, Agarwal NB. Impact of cardiovascular diseases on severity of COVID-19 patients: a systematic review. Ann Acad Med Singapore 2021;50(1):52–60.
[29] Harrison SL, Buckley BJ, Rivera-Caravaca JM, Zhang J, Lip GY. Cardiovascular risk factors, cardiovascular disease, and COVID-19: an umbrella review of systematic reviews. Eur Heart J-Qual Care ClinOutcomes 2021;7(4):330–9.
[30] Clerkin KJ, Justin A, Raikhelkar J, Sayer G, Griffin JM, Masoumi A, et al. COVID-19 and cardiovascular disease. American Heart Association; 2021. p. 1648–55.
[31] Podlubny I. Fractional differential equations. Academic Press, New York; 1999.
[32] Ghaziani RK, Alidousti J, Eshkaftaki AB. Stability and dynamics of a fractional order Leslie–Gower prey-predator model. Appl Math Model 2016;40:2075.
[33] Petras I. Fractional -order nonlinear systems: modeling, analysis and simulation. London, Beijing: Springer; 2011.
[34] Driessche VP, Watmough J. Reproduction numbers and sub-threshold endemic equilibria for compartmentalmodels of disease transmission. Math Biosci 2002;180(2):29–48.
[35] Diekmann O, Heesterbeek JAP, Roberts MG. The construction of next-generation matrices for compartmental epidemic models. J R Soc Interface 2010;7(47):873–85.
[36] Chitnis N, Hyman JM, Cushing JM. Determining important parameters in the spread of malaria through the sensitivity analysis of a mathematical model. Bull Math Biol 2008;70(5):1272.
[37] Vargas-De-León C. Volterra-type Lyapunov functions for fractional-order epidemic systems. Commun Nonlinear Sci Numer Simul 2015;24(3):75–85.
[38] Naik PA, Yavuz M, Zu J. The role of prostitution on HIV transmission with memory: a modeling approach. Alex Eng J 2020;59(4):2513–31.
[39] Jin B, Lazarov R, Zhou Z. An analysis of the L1 scheme for the subdiffusion equation with nonsmooth data. IMA J Numer Anal 2016;36(1):197–221.
[40] Du M, Wang Z. Correcting the initialization of models with fractional derivatives via history-dependent conditions. Acta Mech Sin 2016;2:0–5.
[41] Magin RL. Fractional calculus in bioengineering. Redding: Begell House; 2006.
[42] Diethelm K, Freed AD. The FracPECE subroutine for the numerical solution of differential equations of fractional order. Forsch Wiss Rechnen 1998;1999:57–71.
[43] Diethelm K. An algorithm for the numerical solution of differential equations of fractional order. Electron Trans Numer Anal 1997;5(1):1–6.
[44] Garrappa R. On linear stability of predictor-corrector algorithms for fractional differential equations. Int J Comput Math 2010;87(10):2281–90.
[45] Garrappa R. Numerical solution of fractional differential equations: a survey and a software tutorial. Mathematics 2018;6(2):16.
[46] Li C, Tao C. On the fractional adams method. Comput Math Appl 2009;58(8):1573–88.
[47] Serre R, Benzekry S, Padovani L, Meille C, André N, Ciccolini J, et al. Mathematical modeling of cancer immunotherapy and its synergy with radiotherapy. Cancer Res 2016;76(17):4931–40.